

Renormalization Theory of Stationary Homogeneous Strong Turbulence in a Collisionless Plasma

Yang-zhong Zhang

Institute for Fusion Studies

The University of Texas at Austin

Austin, Texas 78712-1060

(Revised February 1986)

Abstract

A renormalized perturbation theory, as an alternative to the DIA's approach, is presented to describe stationary homogeneous turbulence. The theory can be regarded as a generalization of the resonance broadening theory developed by Dupree, Rudakov-Tsytovich et al., to arbitrary order. Particularly, the incoherent part is treated in a way of matched perturbation theory. The concept of "order" becomes unambiguous by showing renormalizability of the theory. The self-consistency of the theory is manifest owing to the capability of its reduction to the standard results in the limit of weak turbulence as well as to the proof of energy conservation to arbitrary order. For illustrating the amenability of the general framework the renormalized dielectric function and the renormalized Kadomtsev's spectrum equation are derived to second order. The turbulent collisional operator in the transport equations is generally proved equal to Γ_0 , the frequency broadening when $k = 0$.

I. Introduction

It is well known that there exist two different popular approaches in strong turbulence theory for a Vlasov-Poisson system. One is the perturbative approach; the other is the non-perturbative, or functional approach.

The perturbative approach was initiated by Dupree's pioneering work,^{1,2} named "resonance broadening theory", in which the bare propagator $(\omega - \vec{k} \cdot \vec{v})^{-1}$ in the Vlasov equation is intuitively replaced by a renormalized propagator $(\omega - \vec{k} \cdot \vec{v} + i\Gamma_k)^{-1}$. Herein $i\Gamma_k$ stands for the stochastic diffusion arising from the turbulent fields acting on particles.

The later significant progresses along this approach since Dupree's pioneering work consist in the following two points.

- (i) The "single renormalization theory" (as named by Horton and Choi³) is replaced by the "fully renormalized theory", which leads to an equation of $i\Gamma_k$ in terms of the spectrum, instead of its immediate determination through the bare propagator.^{3,4,5}
- (ii) Another term (the β -term as used by Dupree and Tetreault⁶) is added to the non-linear coherent dielectric function (the terminology of coherent dielectric function will be explained in Sec. V) to survive the energy conservation in the electrostatic drift waves, that was violated in the earlier version before Ref. 6).

The modern version of the perturbative approach, typically represented by Refs. 6, 7, and 8 is widely used in physical applications. Among others, Refs. 9 and 10 can be referred.

One problem, which is commonly regarded as a deficiency of the conventional perturbative approach, is how to define the concept of "order". Indeed, this approach has been developed to the second order so far (the order is counted by the number of vertex of wave-particle interaction, [for details, see Appendix A]). Another critique to this approach is related to the following fact that the conventional perturbative theory fails to reduce back to the commonly accepted weak turbulence theory in the corresponding limit, e.g. the well-known Kadomtsev's spectrum equation of weak turbulence (Eq. (II.50) in Ref. 11) does not follow from Dupree's framework even if the turbulence level is very low.

The non-perturbative approach¹² in strong turbulence for a Vlasov-Poisson system can be constructed on the basis of the rigorous MSR (Martin-Siggia-Rose) Systematology.¹³ It is basically a generating functional method for constructing the Green function. However, the system of equations in the MSR systematology contains a functional differential equation of a renormalized vertex Γ . Its rigorous solution seems illusive with present mathematical techniques. In practice one can use the other four equations in the MSR systematology when introducing a rather ad-hoc closure technique of replacing the renormalized vertex Γ by its lowest order approximation – the bare vertex γ , which is a known quantity. This is the DIA (Direct Interaction Approximation).^{12,14,16} Obviously, the DIA has the advantage of keeping the form of the equations in the MSR systematology, although, it is an approximate one. To find a solution of the DIA is not easy. Krommes constructs the DIA equations for Vlasov-Poisson System and proposed the DIAC (Direct Interaction Approximation Coherent) to find a solution in its diffusion approximation and proved the energy conservation of electrostatic drift wave.¹⁷ The approximation used in this solution and the proof of energy conservation are equivalent to the Ref. 6 by Dupree and Tetreault, and that of the second order without the incoherent source of the present paper. A significant success in the DIA's approach is recognized by the capability in reduction to Kadomtsev's weak turbulence equation. Particularly, the dielectric function defined in statistical mechanics^{18,19} is derived in the limit of weak turbulence, and found to be different from the coherent dielectric function used by Dupree.⁶ Besides the diffusion part in the renormalization, the polarization part also contributes to the dielectric function. In a sense this is equivalent to the correlation between the background waves and the induced waves. Therefore, the coherent dielectric function in Dupree's sense is not the dielectric function defined in statistical mechanics, because the contribution from the incoherent part through the correlations mentioned above is ignored.

Although its success in the reduction to weak turbulence theory, the DIA's approach has gone little beyond the perturbative results in physical application to strong turbulence problem. For example, the renormalized version of Kadomtsev's equation (including Compton scattering, nonlinear scattering, and three-wave interactions) and the dielectric function still remain underived from this approach.¹²

Because of its failure in reduction to the weak turbulence theory, the deficiency of Dupree's approach was thought to be due to the ill-treatment of self-consistency for a Vlasov-Poisson equation.¹² This argument might be invoked by the difference in the renormalized propagator used in these two approaches. The propagator used in Dupree's approach only contains the diffusion part, which is related to the self-energy effect, while the propagator used in the MSR systematology and the DIA includes a polarization part also which is related to the polarization cloud around a test particle and to statistical fluctuations in the dielectric response. We shall see in Sec. V that those effects like $\delta f_k(\phi^{(e)})/\delta \phi_{k'}^{(e)}|_{\phi^{(e)}=0}$ for $k \neq k'$ is intrinsically related to the incoherent waves, or more precisely, to the correlation between the background waves and the induced (by the external source) waves. These physical effects do not need to be put in the propagator. The secularity in the bare Green function can be eliminated by self-energy renormalization only. Something like the mass renormalization for Dirac equation. Therefore, if the incoherent part is manipulated correctly in a matched perturbation theory, the physical effects represented by the polarization part will be included in the framework of an alternative theory.

The viewpoint of this paper does not think that the deficiency of Dupree's approach is attributed to the ill treatment of self-consistency. The real problem of Dupree's approach lies in how to develop a matched perturbation theory which can be extended to arbitrary order. The concept of "order" will be elucidated by the renormalizability of the perturbation theory. As we shall see in the latter part of this paper, the deficiency in Dupree's approach should be attributed to the mismatching treatment of incoherent part. As soon as the matched treatment is resumed, the Kadomtsev's weak turbulence equation as well as the dielectric function defined in statistical mechanics will follow correctly from their renormalized versions, which are obtained in this paper and have not been shown in the DIA's approach.

The renormalization procedure presented in this paper is a generalization of Rudakov and Tsytovich's method.⁵ For convenience, a diagrammatical scheme which is introduced in this paper is adopted and illustrated in Appendix A. In dealing with the equation of fluctuating quantities, a formal method, named correlation expansion, is used

to decompose the product of fluctuating quantities into correlated part and uncorrelated part for a general statistical ensemble of turbulence, if no specific knowledge of the correlation probability is presented. Its detailed explanation is given in Appendix B.

The formal solution for the fluctuating distribution functions in a renormalized theory requires the renormalizability of the theory. Hence, the counter term formally added to the equations in accordance with the frequency broadening in the renormalized propagator has to be eliminated in the perturbative expansion of fluctuating distribution function. Otherwise, the fluctuating distribution function would remain in the perturbative expansion of itself as to spoil the significance of the formal solution. The renormalizability thus results in a self-consistent determination of the frequency broadening as well as an elucidation of the concept of "order".

After the renormalization it is shown that f_k can be divided into two parts: the coherent part $f_k^{(c)} = \mathcal{A}_k \phi_k$, and intrinsically incoherent part \tilde{f}_k . It is also shown that the coherent dielectric function $\epsilon_k^{(c)} \equiv 1 - \Phi_k \mathcal{A}_k$, as a generalization of Dupree's definition, is not the dielectric function defined in statistical mechanics. A direct calculation of renormalized dielectric function is given in Sec. V, which is reduced to the result obtained by Krommes and Kleva in the limit of weak turbulence.¹⁸

In the renormalized perturbation theory of this paper the frequency broadening contains the diffusion part only. This statement is valid to arbitrary order [see Sec. VI], where we have shown that the diffusion term in the transport equation is just the frequency broadening at the limit of $k \rightarrow 0$.

In an effort to convince the validity of the proposed propagator the related conservation law should be reviewed. The energy conservation in electrostatic drift waves has been proved to arbitrary order in Sec. VII and explicitly illustrated to the fourth order in Appendix E, beyond second order as current literatures have done.^{6,9,12}

The renormalized version of Kadomtsev's equation is derived in Sec. VIII. It is immediately reduced to the Kadomtsev's equation in the limit of weak turbulence. Therefore, a closed set of spectrum equation to second order is established by the combination of the renormalized Kadomtsev's equation and the frequency broadening equation in Sec. III.

The remainder of this paper is organized as follows. The iterative procedure of

the proposed renormalization is given in Sec. II. The renormalizability is proved and thus the perturbation expansion for the renormalized propagator is obtained in Sec. III. The perturbative form of the coherent dielectric function $\epsilon_k^{(c)}$ and the relevant structure of the intrinsically incoherent function are given in Sec. IV. A few concluding remarks are given in Sec. IX, specifically, the distinctions of the non-perturbative approach based on the MSR systematology to the perturbative approach of this paper are discussed. In Appendix C and D the perturbative expressions for various important structure forms of the theory, which include f_k , the coherent term $f_k^{(c)}$ and the incoherent term \tilde{f}_k are given.

II. Perturbation Theory of Renormalization

For simplicity we study the Vlasov equation without external magnetic and electric fields. We note that the formal structure of the theory is readily generalized. Thus we have

$$\left[\partial_t + \vec{v} \cdot \nabla + (q/m) \vec{E} \cdot \vec{\partial} \right] f(\vec{r}; \vec{v}; t) = 0. \quad (1)$$

Ensemble averaging on Eq. (2) yields

$$(\partial_t + \vec{v} \cdot \nabla) f_0 + (q/m) \langle \vec{E} \cdot \vec{\partial} f' \rangle = 0, \quad (2)$$

where $f_0 \equiv \langle f \rangle$, $f' \equiv f - f_0$, $\langle \dots \rangle$ means the ensemble average.

The equation for the fluctuating distribution function is

$$(\partial_t + \vec{v} \cdot \nabla) f' = -(q/m) \vec{E} \cdot \vec{\partial} f_0 - (q/m) (\vec{E} \cdot \vec{\partial} f')', \quad (3)$$

where

$$(\vec{E} \cdot \vec{\partial} f')' \equiv (\vec{E} \cdot \vec{\partial} f') - \langle \vec{E} \cdot \vec{\partial} f' \rangle$$

is the fluctuating part of $(\vec{E} \cdot \vec{\partial} f')$.

Then taking the Fourier transformation of Eq. (3) and substituting $\vec{E} = -\nabla \phi$ into Eq. (3), yields

$$(\omega - \vec{k} \cdot \vec{v}) f_k = -(q/m) (\vec{k} \cdot \vec{\partial}) f_0 \phi_k \sum_{k_1 \neq k} (q/m) (\vec{k}_1 \cdot \vec{\partial}) \phi_{k_1} f_{k-k_1} (k \neq 0). \quad (4)$$

Now introducing an alternative notation, we have

$$(\omega - \vec{k} \cdot \vec{v}) f_k = \hat{L}(k) f_0 \phi_k + \sum_{k_1 \neq k} \hat{L}(k_1) f_{k-k_1} \phi_{k_1}, \quad (5)$$

where

$$\hat{L}(k) \equiv -(q/m)(\vec{k} \cdot \vec{\partial}).$$

Adding $i\Gamma_k f_k$ on both sides of Eq. (5) (Γ_k is the frequency broadening operator) and defining

$$G_k \equiv (\omega - \vec{k} \cdot \vec{v} + i\Gamma_k)^{-1}. \quad (6)$$

We have

$$f_k = G_k \hat{L}(k) f_0 \phi_k + \sum_{k_1 \neq k} \hat{L}(k_1) f_{k-k_1} \phi_{k_1} + G_k i\Gamma_k f_k. \quad (7)$$

It can be drawn diagrammatically as

$$\text{Diagram 1} = \text{Diagram 2} + \sum_{(k_1)} \text{Diagram 3} + \text{Diagram 4} \quad (8)$$

The precise definition and further discussion of this diagram are given in Appendix A.

The first term on the r.h.s. of Eq. (8) is the lowest order coherent term and the third term containing $i\Gamma_k$ on the r.h.s. of Eq. (8) is the frequency broadening term. On these two terms we cease further iterating. The iteration of the second term on the r.h.s. of Eq. (8) gives

$$\text{Diagram} = \text{Diagram}_1 + \sum_{k_2} \text{Diagram}_2 + \text{Diagram}_3 \quad (9)$$

For a given $\phi_k (k \neq 0)$ which is characteristic of the coherent wave, the waves ϕ_{k_1} and ϕ_{k_2} in the first term on the r.h.s. of Eq. (9) must not be ϕ_k . We call this term the intrinsically incoherent term. The last term of Eq. (19) is the term containing $i\Gamma_k$, for which we also cease to iterate further. The important step at this point is to note that before we make a further iteration on the second term on the r.h.s. of Eq. (9) we need to separate the self-energy structure. The self-energy is just the type of object that $i\Gamma_k$ needs to cancel with.

Such a separation is just the correlation expansion to $\phi_{k_1} \phi_{k_2}$ given in Appendix

B; i.e.,


$$\phi_{k_1} \phi_{k_2} = (\phi_{k_1})(\phi_{k_2}) + \langle\langle \phi_{k_1} \phi_{k_2} \rangle\rangle. \quad (10)$$

Owing to our assumption the nonzero contribution of correlation function $\langle\langle \phi_{k_1} \phi_{k_2} \rangle\rangle$ exists only in case $k_1 + k_2 = 0$. Hence the correlation function can be represented by the closed wiggly lines diagrammatically. The separation of the second term on the r.h.s. of Eq. (10) is thus drawn as

The diagrammatic equation (11) shows a vertex on the left with an incoming straight line from the bottom-left and two outgoing wavy lines labeled k_1 and k_2 . A straight line labeled k also enters the vertex from the top-left. This is set equal to the sum of two terms. The first term is a closed loop (bubble) with wavy lines, with a straight line labeled k entering from the top and another straight line labeled k_1 entering from the bottom. The second term is a vertex with an incoming straight line from the bottom-left and two outgoing wavy lines labeled (k_1) and (k_2) . A straight line labeled k also enters the vertex from the top-left.

$$\text{Diagram 1} = \text{Diagram 2} + \text{Diagram 3} \quad (11)$$

The waves denoted by (k') (with parenthesis!) means they are uncorrelated with each other, while the closed structure (the first term on the r.h.s. of Eq. (11)) represents the correlated part.

Equations (8),(9) and (11) form the renormalized perturbation theory to the second order (counting order by the number of wave-particle interaction vertices excluding the shaded bubble ) when we ask for the cancellations between $-i\Gamma_k$ and the self-energy structure.

(12)

The diagram shows a tadpole diagram (a circle with two external lines) plus a self-energy loop diagram (a circle with two external lines and a loop on top) equals zero.

This is more or less the same theory as given by Rudakov-Tsyтович⁵ and Choi-Horton.²⁰ A crucial point at this step is that we cannot ignore the contribution of the last term in Eq. (11) to this lowest order of renormalization theory. This inclusion is the essential difference between the theory of Dupree-Tetreault⁶ and previous theories. Because the last term of Eq. (11) includes the contribution to the same order, it will be the first term of Eq. (13) shown below as important as the frequency broadening. Its omission can lead to serious error, e.g. in a related driftwave problem it leads to a violation of energy conservation.

The next step goes along the similar line as before with only some additional observations.

The iterations of the last term of Eq. (11) gives

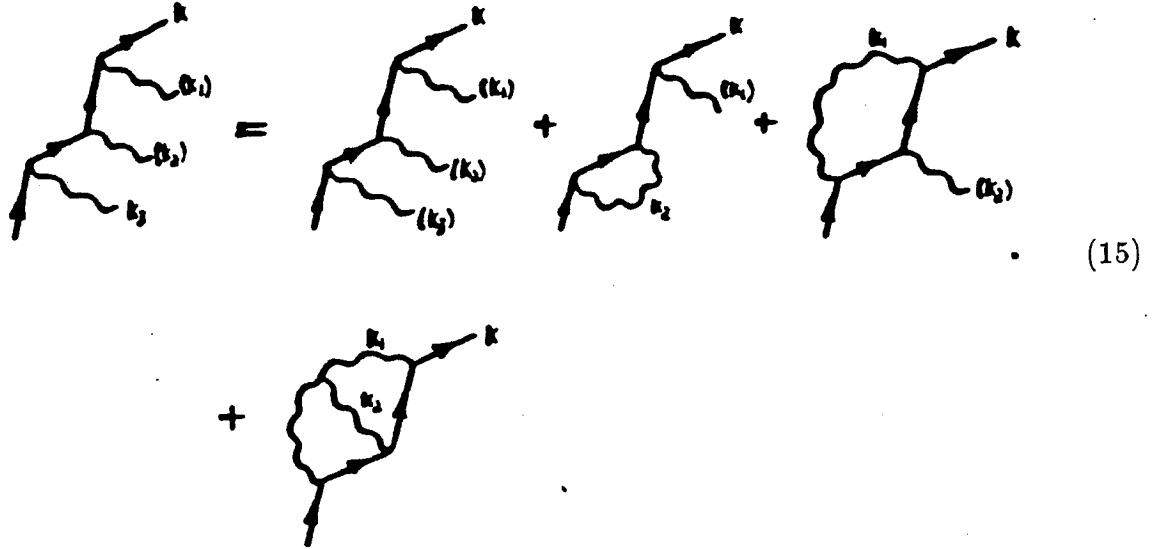
The diagram shows a vertex correction diagram (a circle with two external lines) equal to the sum of three diagrams: a tadpole diagram with a loop, a self-energy loop diagram, and a tadpole diagram with a loop.

(13)

Both the first and the third terms on the r.h.s. of Eq. (13) cease iterating. Further decomposition is needed for the second term before iterating it. This decomposition is just the same as the correlation expansion for $(\phi_{k_2})\phi_{k_3}$, something like that illustrated in Eq. (B9).

$$\begin{aligned} (\phi_{k_1})(\phi_{k_2})\phi_{k_3} &= (\phi_{k_1})(\phi_{k_2})(\phi_{k_3}) + \langle\langle\phi_{k_1}\phi_{k_3}\rangle\rangle(\phi_{k_2}) \\ &\quad + \langle\langle\phi_{k_2}\phi_{k_3}\rangle\rangle(\phi_{k_1}) + \langle\langle\phi_{k_1}\phi_{k_2}\phi_{k_3}\rangle\rangle. \end{aligned} \quad (14)$$

The nonzero contributions from $\langle\langle\phi_{k_1}\phi_{k_2}\phi_{k_3}\rangle\rangle$ exists only if $k_1 + k_2 + k_3 = 0$, as we had argued for $\langle\langle\phi_{k_1}\phi_{k_2}\rangle\rangle$. The decomposition corresponding to Eq. (14) is thus drawn as



$$(15)$$

We note that the second term on the r.h.s. of Eq. (15) cancels the last term on the r.h.s. of Eq. (9), if one uses the expression for the frequency broadening term as obtained to lowest order (which is second order). However, now we need to add to the frequency broadening an additional term and to third order the frequency broadening term is given by

$$- \text{ (circle with two external lines) } = \text{ (diagram 1) } + \text{ (diagram 2) } \quad (16)$$

Now, continuing the iteration, we have

$$\begin{aligned}
 & \text{Diagram 1} = \text{Diagram 2} + \sum_{k_4} \text{Diagram 3} + \text{Diagram 4} \quad (17) \\
 & \text{Diagram 1: A tree diagram with external momenta } k, k_1, k_2, k_3. \\
 & \text{Diagram 2: A tree diagram with external momenta } k, k_1, k_2, k_3 \text{ and an internal loop with momentum } K = k_1 + k_2 + k_3. \\
 & \text{Diagram 3: A tree diagram with external momenta } k, k_1, k_2, k_3 \text{ and an internal loop with momentum } k_4. \\
 & \text{Diagram 4: A tree diagram with external momenta } k, k_1, k_2, k_3 \text{ and an internal loop with momentum } k_4.
 \end{aligned}$$

$$\text{Diagram} = \text{Diagram} + \sum_{k_4} \text{Diagram} + \text{Diagram} \quad (18)$$

The second term on the r.h.s. of Eqs. (17) and (18) need separating. It yields [see Eq. (B9)].

$$\text{Diagram} = \text{Diagram} + \sum_{k_2} \text{Diagram} + \text{Diagram} \quad (19)$$

$$\text{Diagram} = \text{Diagram} + \text{Diagram} \quad (20)$$

The correction to the fourth order for the frequency broadening is thus determined by the eighth term on the r.h.s. of Eq. (19) and the last term of Eq (20). The second term on the r.h.s. of Eq. (19) will cancel the last term of Eq. (13) to this order. To the

appropriate order the fifth term on the r.h.s. of Eq. (19) is the necessary correction for the cancellation between the last term of Eq. (19) and the second term on the r.h.s. of Eq. (15).

Except those self-energy terms all other terms in Eqs. (19) and (20) should be iterated to produce the next order.

The general rules for the perturbative expansion is summarized as follows:

- (a) The terms containing shaded bubble, the self-energy terms and the frequency broadening terms (which contain a hollow bubble) will be kept without further manipulation but the cancellation between the last two sorts of terms.
- (b) When a term which does not belong to anyone in the above terms contains an external wiggly line without parenthesis, it needs separating according to the correlation expansion.
- (c) After the separation those terms which do not contain a self-energy structure need iterating to produce the next order. We shall prove that these will be an exact cancellation between terms containing self-energy structure and terms containing frequency broadening and the final result for f_k is illustrated in Appendix C diagrammatically to the fifth order.

III. Renormalizability

The statement in Sec. II implies that all terms containing self-energy structure cancel with all the terms containing frequency broadening so that none of these terms explicitly appear in the final expression of f_k . By virtue of this cancellation, we will show that $i\Gamma_k$ is determined as the sum of all possible irreducible self-energy structures taken once and only once. We note that the definition of renormalizability means that if $i\Gamma_k$ can be expressed as the sum of self-energy terms, that all diagrams containing self-energy and frequency broadening sub-structures will cancel with each other.

We first discuss in detail several properties that manifest themselves as results of our iteration procedures.

Observation I. At a given order all possible self-energy structures must appear except those (and never those) that contain self-energy sub-structures. (Henceforth, the allowable self-energy structure will be called to a completely overlapping diagram in which no self-energy sub-structures can be isolated.)

Proof. According to the iteration rule indicated in Sec. II, when a simple self-energy diagram once appears, further iteration of the diagram ceases. This means that any term in higher order does not contain the self-energy structure of lower order. In other words the allowable self-energy structure can only be formed by connecting the lowest wiggly line (we refer to it as the active line) with the upper lines (we refer to them as the passive lines). Because no self-energy structure can appear above the active line, the connection can only produce the completely overlapping diagram.

In order to show that all types of completely overlapping patterns are possible, we need only note that all types of vertex structures are possible in the terms of lower order because the operation $k_i \rightarrow (k_i)$ makes each active line connect with every possible combination of passive lines. Therefore, all types of self-energy structure should be taken into account except those containing the lower order self-energy structure as a sub-diagram.

According to Observation I, the following diagrams are examples of structures that should be excluded from the contributor as self-energy diagram (Fig. 1).

Observation II. A given diagram can only appear once. There is no repeated diagram.

Proof. All terms appearing in the theory can only be produced in two ways. One is the iteration, the other is the separation (i.e., the operation $k_i \rightarrow (k_i)$). The iteration cannot produce a repeated diagram. In the operation $k_i \rightarrow (k_i)$ only the lower wiggly line is active (the word "active" meaning that the lower line can correlate with any other passive wiggly lines). In contrast, the passive lines, for which the momenta have been denoted by (k_i) cannot be correlated with any wiggly line but the active one. Hence, new diagrams can only be formed from the active part by connecting only to the lowest line. This kind of diagram certainly does not appear in the previous order.

Observation III. For non-self-energy diagrams containing self-energy sub-structure all types of self-energy structure produced in the lower perturbative order are reproduced totally in the higher perturbative order.

Proof. All possible types of self-energy structure are produced by the operation $k_i \rightarrow (k_i)$ of the lowest wiggly line. The operation in the higher order repeats in the lower order as well as adding new ones. Because the structure in the iteration goes in the downward direction and repeats all lower order diagram of each iteration, the same operation that appeared in the lower orders must appear in higher order regardless of the structure in the upper part of the diagrams.

Observation IV. In the higher perturbative order diagrams there exists no new type of self-energy sub-structure which has the same order as the self-energy structure that has already appeared in a lower perturbative order diagram.

Proof. Owing to the Observation I, the self-energy structure to the given order cannot go beyond that given by all types of completely overlapping structure. The self-energy structures appearing in the lower perturbative orders have completed all possibilities to the corresponding order of self-energy diagram.

It is then straightforward with the help of these four observations to prove the renormalizability of the theory and to obtain the general form of the renormalized propagator to any order.

The Observation I suggests the choice of $-i\Gamma_k$ to be the sum of all types of possible self-energy structures. The combination of the Observation II, III and IV means that as soon as the cancellation takes place for the lowest order diagram containing $i\Gamma_k$, the same

cancellation occurs for the higher order diagrams that have structure plus $i\Gamma_k$ with the diagram with that structure plus all self-energy structures.

The explicit diagrammatical expression of $i\Gamma_k$ to the sixth order is given as follows, where the iterative order of each diagram is readily recognized by counting number of vertices of the diagram.

$$\begin{aligned}
 -i\Gamma_k = & \text{diagram 1} + \text{diagram 2} + \text{diagram 3} + \text{diagram 4} \\
 & + \text{diagram 5} + \text{diagram 6} + \text{diagram 7} + \text{diagram 8} \\
 & + \text{diagram 9} + \text{diagram 10} + \text{diagram 11} + \text{diagram 12} \\
 & + \text{diagram 13} + \text{diagram 14} + \text{diagram 15} + \text{diagram 16} \\
 & + \text{diagram 17} + \text{diagram 18} + \text{diagram 19} + \text{diagram 20} \\
 & + \text{diagram 21} + \text{diagram 22} + \text{diagram 23} + \text{diagram 24} \\
 & + \text{diagram 25} + \text{diagram 26} + \dots
 \end{aligned}
 \tag{21}$$

The Green function G_k and $i\Gamma_k$, the latter is expressed in terms of correlation function $\langle\langle\phi_{k_1}\dots\rangle\rangle$ and G_k given in Eq. (21), are coupled together to ensure the non-fluctuating property of G_k . From these coupling relations we readily infer that both G_k and $i\Gamma_k$ are complex, i.e., besides the frequency broadening of $i\Gamma_k$ there must be a frequency shift (being a nonlinear shift) caused by the renormalization.

IV. Coherent and Intrinsically Incoherent Distribution Functions

Now we are going to manipulate the perturbative expression of f_k further because the wiggly line pertaining to the shaded bubble may be still correlated with other open wiggly lines in a given diagram.

It is easily seen that the first terms on the r.h.s. of Eqs. (8) and (9) retain their form. The first term on the r.h.s. of Eq. (13) becomes

$$\text{Diagram 1} = \text{Diagram 2} + \text{Diagram 3} \quad (22)$$

The diagram obtained by connecting the wiggly line of ϕ_{k_2} with the wiggly line $\phi_{k-k_1-k_2}$ is not present. It requires the propagator corresponding to the solid line (a) of the figure have zero momentum, which cannot be produced in the iteration procedure. The first term on the r.h.s. of Eq. (22) is the coherent term to the second order of the perturbation theory, because all parts of this term except ϕ_k belong to the non-fluctuating effect. The last term of Eq. (22) is the intrinsically incoherent term to second order, i.e., any wiggly line in this term cannot be assigned a momentum ϕ_k , for such an assignment will result in an excluded diagram. For example, if we assign the wiggly line under the shaded bubble a momentum k , it will force $k_1 = -k_2$ which is an excluded choice for the last diagram in Eq. (22), owing to the separation of the self-energy term in Eq. (11). Thus

we can conclude that none of the wiggly lines can have a momentum k in a diagram with all wiggly lines uncorrelated to each other.

Because the lowest order of the renormalization occurs to at least the second order, we must include the corresponding second order to have a consistent theory. As can be easily seen, the first term on the r.h.s. of Eq. (22) is just the β -term proposed by Dupree and Tetreault⁶ to retain the conservation of energy in a related formulism for the driftwave problem.

In third order the term of f_k after the renormalization cancellation in Eq. (17) becomes

$$\text{Diagram 1} = \text{Diagram 2} + \text{Diagram 3} + \text{Diagram 4} + \text{Diagram 5} + \text{Diagram 6} + \text{Diagram 7} \quad (23)$$

The first two terms on the r.h.s. of Eq. (23) are coherent terms, the last three terms on the r.h.s. of Eq. (23) are intrinsically incoherent terms.

The first term for f_k in Eq. (18) is an intrinsically incoherent term, because the setting of $k - k_2 = k$ or $k_2 = k$ gives zero contributions to this diagram.

Going along this line we readily obtain the result that the fluctuating function is divided into a coherent part and an intrinsically incoherent part

$$f_k = f_k^{(c)} + \tilde{f}_k \quad (24)$$

where $f_k^{(c)}$ represents all coherent terms, and \tilde{f}_k represents all incoherent terms. To third order of perturbation they are expressed diagrammatically as

$$f_k^{(c)} = \text{diagram 1} + \text{diagram 2} + \text{diagram 3} + \text{diagram 4} + \dots \quad (25)$$

$$\tilde{f}_k = \text{diagram 1} + \text{diagram 2} + \text{diagram 3} + \text{diagram 4} + \dots \quad (26)$$

Their perturbative expressions to fifth order and the general construction rules in terms of diagrammatics are given in Appendix D.

The coherent part can be expressed as $f_k^{(c)} = \mathcal{A}_k \phi_k$, where \mathcal{A}_k represents the non-fluctuating effect. We define an operator Φ_k :

$$\Phi_k \equiv -\frac{4\pi q}{|\vec{k}|^2} \int d\vec{v}. \quad (27)$$

The Poisson equation is written as

$$\phi_k = \Phi_k f_k. \quad (28)$$

When substituting Eq. (24) into Eq. (28) we obtain

$$\epsilon_k^{(c)} \phi_k = \Phi_k \tilde{f}_k \equiv \tilde{\phi} \quad (29)$$

where

$$\epsilon_k^{(c)} \equiv 1 - \Phi_k \mathcal{A}_k. \quad (30)$$

For the historical sake $\epsilon_k^{(c)}$ is called renormalized dielectric function, because it was thought to be the dielectric function incorrectly.

Starting from the renormalized coherent dielectric function $\epsilon_k^{(c)}$ the renormalized average distributions function \bar{f}_k can be defined as

$$\epsilon_k^{(c)} \equiv 1 - \Phi_k G_k \hat{L}(k) \bar{f}_k \quad (31)$$

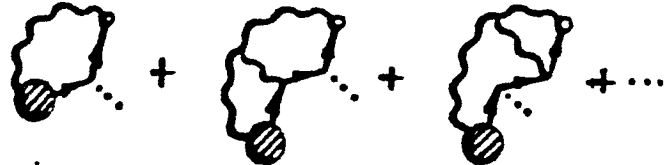
which is motivated from the form of the linear dielectric function $\epsilon_k^{(\ell)}$ given by

$$\epsilon_k^{(\ell)} \equiv 1 - \Phi_k G_k^{(0)} \hat{L}(k) f_0. \quad (32)$$

The definition of \bar{f}_k by Eq. (31) is somewhat different from that defined in Ref. 12 and 19, where $\epsilon_k^{(c)}$ is replaced by ϵ_k , the dielectric function in statistical physics. The renormalized average distribution function \bar{f}_k can be written as

$$\hat{L}(k) \bar{f}_k = G_k^{-1} \mathcal{A}_k. \quad (33)$$

As $G_k^{-1} \mathcal{A}$ just annihilates all upper line of the \mathcal{A} diagram, the perturbative expansion of \bar{f}_k is given by

$$\bar{f}_k = \hat{L}(k) G_k^{-1} \mathcal{A}_k = f_0 + \text{diagram 1} + \text{diagram 2} + \text{diagram 3} + \dots \quad (34)$$


where the denotation o implies the missing vertex $\hat{L}(k)$. We note, however, that the utility of \bar{f}_k is somewhat limited as its velocity moments do not have any apparent physical significance.

V. Inverse Dielectric Function

The renormalized perturbation theory can be used to calculate the inverse dielectric function ϵ^{-1} .

In the electrostatic wave it is defined through Poisson equation:¹⁸

$$\epsilon_k^{-1} = \frac{\vec{k}^2}{4\pi} \frac{\delta \langle \phi_k(\phi^{(e)}) \rangle}{\delta \rho_k^{(e)}} \quad (35)$$

where $\rho^{(e)}$ is the unrandom external source. The response to the bare source is $\phi_k^{(e)} = (4\pi/|\vec{k}|^2)\rho_k^{(e)}$. Thus we have

$$\epsilon_k^{-1} = 1 + \Phi_k \left\langle \frac{\delta f_k(\phi^{(e)})}{\delta \phi_k^{(e)}} \right\rangle_{\phi^{(e)}=0} \quad (36)$$

The Vlasov equation becomes

$$\left[\partial_t + \vec{v} \cdot \nabla + (q/m) \vec{E}(\vec{E}^{(e)}) \cdot \vec{\partial} \right] f(\vec{E}^{(e)}) = 0. \quad (37)$$

The Poisson equation is

$$\phi_k(\phi^{(e)}) = \phi_k^{(e)} + \Phi_k f_k(\phi^{(e)}). \quad (38)$$

For an infinitesimal external source $\delta \phi_k^{(e)}$

$$\phi_k(\phi^{(e)}) \rightarrow \phi_k(0) + \left[\delta_{kk'} + \Phi_k \left(\frac{\delta f_k(\phi^{(e)})}{\delta \phi_{k'}^{(e)}} \right)_{\phi^{(e)}=0} \right] \delta \phi_{k'}^{(e)} \quad (39)$$

where $\phi_k(0) = \Phi_k f_k(\phi^{(e)}) \Big|_{\phi^{(e)}=0}$.

Equation (39) shows that the variation of ϕ under the influence of external field $\delta \phi_k^{(e)}$ is

$$\delta \phi_k = \left[\delta_{kk'} + \Phi_k \left(\frac{\delta f_k(\phi^{(e)})}{\delta \phi_{k'}^{(e)}} \right)_{\phi^{(e)}=0} \right] \delta \phi_{k'}^{(e)}. \quad (40)$$

When defining $f_0 \equiv \langle f(\phi^{(e)}=0) \rangle$ and $f(\phi^{(e)}) \equiv f_0 + f'(\phi^{(e)})$ we have for the Fourier transformation of Eq. (37) for $k \neq 0$

$$f'_k(\delta\phi^{(e)}) =$$

$$+ \sum_{(a_1)} \text{diagram} + \sum_{(a_1)} \text{diagram} + \text{diagram}$$

(41)

where the wiggly lines represent $\phi_k(0)$, the dashed lines represent $\delta\phi_k$. The iteration procedure for $f_k(\delta\phi^{(e)})$ should be modified a little bit. Because the external source $\delta\phi^{(e)}$ makes sense only in its linear form, the operation $k_i \rightarrow (k_i)$ only limits choices of the stochastic field ϕ rather than $\phi^{(e)}$. Therefore, the dashed lines representing the effect of the external source $\delta\phi_k^{(e)}$ can only be external lines. This suggests that if the lowest wiggly line is the external source, the corresponding term should be iterated further. On the other hand if more than one dashed line appear in a diagram, the contribution of the diagram to the final result $\left\langle \delta f_k(\phi^{(e)}) / \delta\phi_k^{(e)} \right\rangle_{\phi^{(e)}=0}$ vanishes and we drop these diagrams. The renormalization in this case is almost the same as what has been described in the renormalization of Sec. II. The first few steps of this iteration procedure are illustrated in the following. In Eq. (41) only the third term on the r.h.s. of the equation needs to be iterated further, yielding

$$\begin{array}{c} \diagup \\ \diagdown \end{array} k_1 = \begin{array}{c} \diagup \\ \diagdown \end{array} k_1 + \sum_{k_2} \begin{array}{c} \diagup \\ \diagdown \end{array} k_1 + \sum_{k_2} \begin{array}{c} \diagup \\ \diagdown \end{array} k_1 + \begin{array}{c} \diagup \\ \diagdown \end{array} k_1 \quad (42)$$

Before iterating the second term on the r.h.s. of Eq. (42) we separate the correlation part, obtaining

$$\begin{array}{c} \diagup \\ \diagdown \end{array} k = \begin{array}{c} \diagup \\ \diagdown \end{array} k + \begin{array}{c} \diagup \\ \diagdown \end{array} (k_1) \quad (43)$$

where the last term of Eq. (43) should be iterated.

$$\begin{array}{c} \diagup \\ \diagdown \end{array} k = \begin{array}{c} \diagup \\ \diagdown \end{array} k + \sum_{k_2} \begin{array}{c} \diagup \\ \diagdown \end{array} k + \sum_{k_2} \begin{array}{c} \diagup \\ \diagdown \end{array} k + \begin{array}{c} \diagup \\ \diagdown \end{array} k \quad (44)$$

The third term on the r.h.s. of Eq. (42) needs no separating and gives

$$\begin{array}{c} k \\ \diagup \\ \text{---} \\ \diagdown \\ k_1 \\ \text{---} \\ k_2 \end{array} = \begin{array}{c} k \\ \diagup \\ \text{---} \\ \diagdown \\ k_1 \\ \text{---} \\ k_2 \end{array} + \sum_{k_3} \begin{array}{c} k \\ \diagup \\ \text{---} \\ \diagdown \\ k_1 \\ \text{---} \\ k_3 \end{array} + \begin{array}{c} k \\ \diagup \\ \text{---} \\ \diagdown \\ k_1 \\ \text{---} \\ k_2 \end{array} \quad (45)$$

The second term on the r.h.s. of Eq. (44) needs separating before iteration, while the third term on the r.h.s. of Eq. (44) and the second term on the r.h.s. of Eq. (45) can be iterated directly. Hence we have

$$\begin{array}{c} k \\ \diagup \\ \text{---} \\ \diagdown \\ k_1 \\ \text{---} \\ k_2 \end{array} = \begin{array}{c} k \\ \diagup \\ \text{---} \\ \diagdown \\ k_1 \\ \text{---} \\ k_2 \end{array} + \begin{array}{c} k \\ \diagup \\ \text{---} \\ \diagdown \\ k_1 \\ \text{---} \\ k_2 \end{array} + \begin{array}{c} k \\ \diagup \\ \text{---} \\ \diagdown \\ k_1 \\ \text{---} \\ k_2 \end{array} + \begin{array}{c} k \\ \diagup \\ \text{---} \\ \diagdown \\ k_1 \\ \text{---} \\ k_2 \end{array} \quad (46)$$

$$\begin{array}{c} k \\ \diagup \\ \text{---} \\ \diagdown \\ k_1 \\ \text{---} \\ k_2 \end{array} = \begin{array}{c} k \\ \diagup \\ \text{---} \\ \diagdown \\ k_1 \\ \text{---} \\ k_2 \end{array} + \sum_{k_3} \begin{array}{c} k \\ \diagup \\ \text{---} \\ \diagdown \\ k_1 \\ \text{---} \\ k_3 \end{array} + \sum_{k_3} \begin{array}{c} k \\ \diagup \\ \text{---} \\ \diagdown \\ k_1 \\ \text{---} \\ k_3 \end{array} + \begin{array}{c} k \\ \diagup \\ \text{---} \\ \diagdown \\ k_1 \\ \text{---} \\ k_2 \end{array} \quad (47)$$

$$\begin{array}{c} k \\ \diagup \\ \text{---} \\ \diagdown \\ k_1 \\ \text{---} \\ k_2 \end{array} = \begin{array}{c} k \\ \diagup \\ \text{---} \\ \diagdown \\ k_1 \\ \text{---} \\ k_2 \end{array} + \sum_{k_3} \begin{array}{c} k \\ \diagup \\ \text{---} \\ \diagdown \\ k_1 \\ \text{---} \\ k_3 \end{array} + \begin{array}{c} k \\ \diagup \\ \text{---} \\ \diagdown \\ k_1 \\ \text{---} \\ k_2 \end{array} \quad (48)$$

$$\begin{array}{c} k \\ \diagup \\ \text{---} \\ \diagdown \\ k_1 \\ \text{---} \\ k_2 \end{array} = \begin{array}{c} k \\ \diagup \\ \text{---} \\ \diagdown \\ k_1 \\ \text{---} \\ k_2 \end{array} + \sum_{k_3} \begin{array}{c} k \\ \diagup \\ \text{---} \\ \diagdown \\ k_1 \\ \text{---} \\ k_3 \end{array} + \sum_{k_3} \begin{array}{c} k \\ \diagup \\ \text{---} \\ \diagdown \\ k_1 \\ \text{---} \\ k_3 \end{array} + \begin{array}{c} k \\ \diagup \\ \text{---} \\ \diagdown \\ k_1 \\ \text{---} \\ k_2 \end{array} \quad (49)$$

$$\begin{array}{c} k \\ \diagup \\ \text{---} \\ \diagdown \\ k_1 \\ \text{---} \\ k_2 \end{array} = \begin{array}{c} k \\ \diagup \\ \text{---} \\ \diagdown \\ k_1 \\ \text{---} \\ k_2 \end{array} + \begin{array}{c} k \\ \diagup \\ \text{---} \\ \diagdown \\ k_1 \\ \text{---} \\ k_2 \end{array} + \sum_{k_3} \begin{array}{c} k \\ \diagup \\ \text{---} \\ \diagdown \\ k_1 \\ \text{---} \\ k_3 \end{array} + \begin{array}{c} k \\ \diagup \\ \text{---} \\ \diagdown \\ k_1 \\ \text{---} \\ k_2 \end{array} \quad (50)$$

$$\begin{aligned}
& \text{Diagram 1} = \text{Diagram 2} + \text{Diagram 3} + \text{Diagram 4} + \text{Diagram 5} \\
& + \text{Diagram 6} + \text{Diagram 7} + \text{Diagram 8} + \text{Diagram 9}
\end{aligned}
\tag{51}$$

and further iteration gives

The separation for the second terms on the r.h.s. of Eqs. (47), (48) and (50) yields

$$\text{Diagram 1} = \text{Diagram 2} + \text{Diagram 3} + \text{Diagram 4}
\tag{52}$$

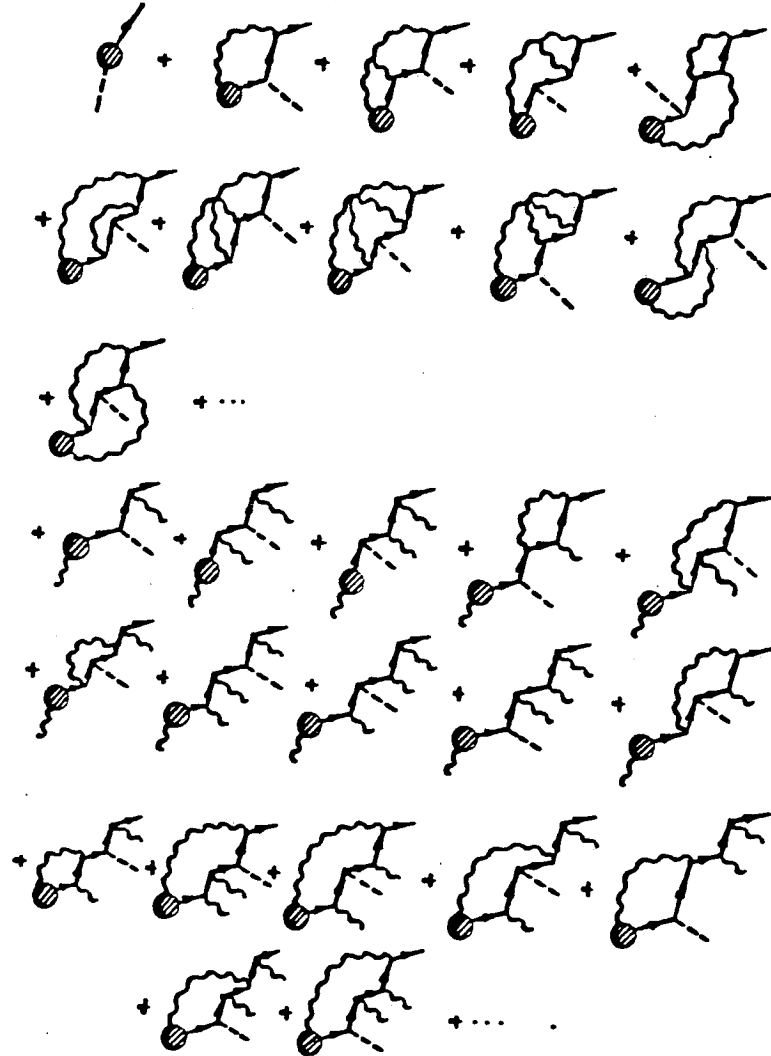
$$\text{Diagram 1} = \text{Diagram 2} + \text{Diagram 3} + \text{Diagram 4}
\tag{53}$$

This procedure can go along up to higher orders and will demonstrate the full cancellation between frequency broadening terms and the self-energy structure terms. The proof of the renormalizability is the same as what was given in Sec. III. The appearance of dashed line does not affect the renormalizability as shown by the cancellation between first terms on the r.h.s. of Eq. (53) and the last term of Eq. (45). After the full cancellation between frequency broadening terms and the terms containing self-energy structure the remaining terms can be divided into two parts. One part is just the $f_k(0)$, in which no dashed line appears. The other part is composed of terms which contain only one dashed line. Their formation rule can be summarized as follows. Starting from the fundamental constructive diagrams (see Appendix D), each external wiggly line is replaced by dashed line only once in a given fundamental constructive diagram; the total sum of the resultant

diagram is the second part, if such a replacement does not cause a zero-momentum propagator or a self-energy structure when the momentum of the dashed line is taken to be k . Thus

$$f_k(\delta\phi^{(e)}) = f_k(0) + (\text{fundamental constructive diagrams})_{\text{open}} \phi_k \rightarrow \delta\phi_k. \quad (54)$$

The perturbative expressions of $\delta f_k(\delta\phi^{(e)}) = f_k(\delta\phi^{(e)}) - f_k(0)$ to the fourth order are illustrated as follows:


(55)

Then we have the general formula

$$(1 - \Phi_k \mathcal{A}_k) \Phi_k \frac{\delta f_k}{\delta \phi_{k'}^{(e)}} = \Phi_k \mathcal{A}_k \delta_{kk'} + \Phi_k \tilde{f}_k \left| \phi_{k_i} \rightarrow \delta_{k_i k'} + \Phi_{k_i} \frac{\delta f_{k_i}}{\delta \phi_{k'}^{(e)}}. \quad (56)$$

The formal solution of inverse dielectric function ϵ_k^{-1} is thus found to be

$$\begin{aligned}\epsilon_k^{-1} &= 1 + \phi_k \left\langle \frac{\delta k_k}{\delta \phi_k^{(e)}} \right\rangle_{\phi^{(e)}=0} \\ &= \langle Q_{kk}^{-1} \rangle \Phi_k \mathcal{A}_k + \sum_{k_i} \left\langle Q_{kk_i}^{-1} \Phi_{k_i} \tilde{f}_{k_i} \left| \phi_{k_j} \rightarrow \delta_{k_j k} \right. \right\rangle\end{aligned}\quad (57)$$

where $Q_{k_i k_j}^{-1}$ is the inverse matrix of $Q_{k_i k_j}$ with

$$Q_{k_i k_j} \equiv (1 - \Phi_{k_i} \mathcal{A}_{k_i}) \delta_{k_i k_j} - P_{k_i k_j} \quad (58)$$

and $P_{k_i k_j}$ is defined by

$$\sum_{k_j} P_{k_i k_j} \Phi_{k_j} \frac{\delta f_{k_j}}{\delta \phi_{k'}^{(e)}} \equiv \Phi_{k_i} \tilde{f}_{k_i} \left| \phi_j \rightarrow \Phi_{k_j} (\delta f_{k_j} / \delta \phi_{k'}^{(e)}) \right. \quad (59)$$

To the second order $P_{k_i k_j}$ is shown below diagrammatically,

$$\begin{aligned}P_{k_i k_j} = \Phi_{k_i} \left\{ \right. & \begin{array}{c} \text{Diagram 1: } \text{A shaded circle with an incoming wavy line from the bottom labeled } k_i - k_j. \text{ Two outgoing wavy lines from the top: one labeled } k_i \text{ and the other } k_j. \end{array} \\ & + \begin{array}{c} \text{Diagram 2: } \text{A shaded circle with an incoming wavy line from the bottom labeled } k_j. \text{ Two outgoing wavy lines from the top: one labeled } k_i \text{ and the other } k_i - k_j. \end{array} \\ & + \begin{array}{c} \text{Diagram 3: } \text{A shaded circle with an incoming wavy line from the bottom labeled } k_i - k_j - k_2. \text{ Two outgoing wavy lines from the top: one labeled } k_i \text{ and the other } k_j. \end{array} \\ & + \begin{array}{c} \text{Diagram 4: } \text{A shaded circle with an incoming wavy line from the bottom labeled } k_i - k_1 - k_j. \text{ Two outgoing wavy lines from the top: one labeled } k_i \text{ and the other } k_j. \end{array} \\ & + \begin{array}{c} \text{Diagram 5: } \text{A shaded circle with an incoming wavy line from the bottom labeled } k_j. \text{ Two outgoing wavy lines from the top: one labeled } k_i \text{ and the other } k_i - k_1 - k_j. \end{array} \left. \right\} \quad (60)\end{aligned}$$

In a demonstration of the amenability of the perturbative calculation for the renormalized dielectric function ϵ_k , an illustration to second order is shown below.

Setting $k' = k$ in Eq. (56), to second order we have

$$\Phi_k \frac{\delta f_k}{\delta \phi_k^{(e)}} = \left(\epsilon_k^{(c)-1} - 1 \right) + \epsilon_k^{(c)-1} \Phi_k \left\{ \begin{array}{c} \text{diagram: } k \text{ entering a shaded circle, } k_1 \text{ entering from below, } k-k_1 \text{ exiting to the left} \\ \text{diagram: } k \text{ entering a shaded circle, } k_1 \text{ entering from below, } k-k_1 \text{ exiting to the right} \end{array} \right\} \Phi_{k-k_1} \frac{\delta f_{k-k_1}}{\delta \phi_k^{(e)}} + \begin{array}{c} \text{diagram: } k \text{ entering a shaded circle, } k_1 \text{ entering from below, } k-k_1 \text{ exiting to the left} \\ \text{diagram: } k \text{ entering a shaded circle, } k_1 \text{ entering from below, } k-k_1 \text{ exiting to the right} \end{array} \Phi_{k_1} \frac{\delta f_{k_1}}{\delta \phi_k^{(e)}} \right\} \quad (61)$$

where

$$\epsilon_k^{(c)} \equiv 1 - \Phi_k \mathcal{A} \xrightarrow{\text{to second order}} 1 - \Phi_k \left\{ \begin{array}{c} \text{diagram: } k \text{ entering a shaded circle, } k \text{ exiting to the left} \\ \text{diagram: } k \text{ entering a shaded circle, } k \text{ entering from below, } k \text{ exiting to the right} \end{array} \right\} = 1 + \frac{4\pi q}{|\vec{k}|^2} \int d\vec{v} G_k \left[\hat{L}(k) + \sum_{k_1} \hat{L}(k_1) G_{k-k_1} \hat{L}(k) G_{-k_1} \hat{L}(-k_1) I_{k_1} \right] f_0 \quad (62)$$

with $I_{k_1} \equiv \langle \phi_{k_1} \phi_{k_1}^* \rangle$.

Those terms like $\epsilon_k^{(e)-1} \Phi_k \begin{array}{c} \text{diagram: } k \text{ entering a shaded circle, } k_1 \text{ entering from below, } k_2 \text{ entering from below, } k-k_1-k_2 \text{ exiting to the left} \end{array} \Phi_{k-k_1-k_2} \frac{\delta f_{k-k_1-k_2}}{\delta \phi_k^{(e)}}$ do not contribute to the second order because ϕ_{k_1} and ϕ_{k_2} are uncorrelated.

An iteration to the $\delta f_{k_1}/\delta \phi_k^{(e)}$ and $\delta f_{k-k_1}/\delta \phi_k^{(e)}$ in Eq. (61) to second order gives

$$\Phi_{k_1} \frac{\delta f_{k_1}}{\delta \phi_k^{(e)}} = \epsilon_{k_1}^{(c)-1} \Phi_{k_1} \left\{ \begin{array}{c} \text{diagram: } k_1 \text{ entering a shaded circle, } k_1-k \text{ entering from below, } k_1-k \text{ exiting to the left} \\ \text{diagram: } k_1 \text{ entering a shaded circle, } k_1-k \text{ entering from below, } k_1-k \text{ exiting to the right} \end{array} \right\} \epsilon_k^{(c)-1} + \begin{array}{c} \text{diagram: } k_1 \text{ entering a shaded circle, } k_1-k \text{ entering from below, } k_1-k \text{ exiting to the left} \\ \text{diagram: } k_1 \text{ entering a shaded circle, } k_1-k \text{ entering from below, } k_1-k \text{ exiting to the right} \end{array} \epsilon_k^{(c)-1} \quad (63)$$

$$\Phi_{k-k_1} \frac{\delta f_{k-k_1}}{\delta \phi_k^{(e)}} = \epsilon_{k-k_1}^{(c)-1} \Phi_{k-k_1} \left\{ \begin{array}{c} \text{diagram: } k-k_1 \text{ entering a shaded circle, } -k_1 \text{ entering from below, } k-k_1 \text{ exiting to the left} \\ \text{diagram: } k-k_1 \text{ entering a shaded circle, } -k_1 \text{ entering from below, } k-k_1 \text{ exiting to the right} \end{array} \right\} \epsilon_k^{(c)-1} + \begin{array}{c} \text{diagram: } k-k_1 \text{ entering a shaded circle, } -k_1 \text{ entering from below, } k-k_1 \text{ exiting to the left} \\ \text{diagram: } k-k_1 \text{ entering a shaded circle, } -k_1 \text{ entering from below, } k-k_1 \text{ exiting to the right} \end{array} \epsilon_k^{(c)-1}. \quad (64)$$

Then we obtain

$$\epsilon_k^{-1} = 1 + \Phi_k \left\langle \frac{\delta f_k}{\delta \phi_k^{(e)}} \right\rangle_{\phi^{(e)}=0} = \epsilon_k^{(c)-1} + 4\epsilon_k^{(c)-1} \tilde{\epsilon}_{k_1, k-k_1}^{(2)} \epsilon_{k-k_1}^{(c)-1} \tilde{\epsilon}_{-k_1, k}^{(2)} \epsilon_k^{(c)-1} I_{k_1} \quad (65)$$

where

$$\tilde{\epsilon}_{k_1, k_2}^{(2)} \equiv \frac{1}{2} \phi_{k_1+k_2} \left[\begin{array}{c} \text{diagram: } k_1+k_2 \text{ entering a shaded circle, } k_1 \text{ entering from below, } k_2 \text{ entering from below} \\ \text{diagram: } k_1+k_2 \text{ entering a shaded circle, } k_2 \text{ entering from below, } k_1 \text{ entering from below} \end{array} \right] = -\frac{1}{2} \frac{4\pi q}{|\vec{k}_1 + \vec{k}_2|^2} \int d\vec{v} G_{k_1+k_2} \left[\hat{L}(k_1) G_{k_2} \hat{L}(k_2) + \hat{L}(k_2) G_{k_1} \hat{L}(k_1) \right] f_0. \quad (66)$$

VI. Transport Equation

The complete transport equation in the renormalization formulism should be written as [see Eq. (2)]

$$(\partial_t + \vec{v} \cdot \nabla) f_0 + i(q/m) \sum_k (\vec{k} \cdot \vec{\partial}) \left[\mathcal{A} \langle \phi_k^* \phi_k \rangle + \langle \phi_k^* \tilde{f}_k \rangle \right] = 0. \quad (72)$$

In order to get a neat form of the turbulent collisional operator,

$$i(q/m) \sum_k (\vec{k} \cdot \vec{\partial}) \left[\mathcal{A} \langle \phi_k^* \phi_k \rangle + \langle \tilde{f}_k \phi_k^* \rangle \right],$$


we study its diagrammatical structure.

When we note $\hat{L}(k) = -(q/m)(\vec{k} \cdot \vec{\partial})$, the turbulent collisional operator can be written as a series of connected diagrams. A few terms are illustrated as follows

$$\sum_{kk} \hat{L}(k) \mathcal{A} \langle \phi_k \phi_k^* \rangle = \text{[Diagram 1]} + \text{[Diagram 2]} + \text{[Diagram 3]} + \text{[Diagram 4]} + \dots \quad (73)$$

$$\sum_k \hat{L}(k) \cdot \langle \tilde{f}_k \phi_k^* \rangle = \text{[Diagram 5]} + \text{[Diagram 6]} + \text{[Diagram 7]} + \text{[Diagram 8]} + \text{[Diagram 9]} + \dots \quad (74)$$

where the perturbative expressions of $f_k^{(c)}$ and \tilde{f}_k (Appendix D) have been used in writing down Eqs. (73) and (74).

We recall the shaded bubble  $= \hat{L}(k') f_0$, where k' is the momentum of the solid line just above the bubble. For the time being, in order to study the diagrammatic structure of Eqs. (73) and (74), we extract f_0 from the bubble. Thus Eqs. (73) and (74) become

$$\begin{aligned}
\sum_k \hat{L}(k) \langle \phi_k^* f_k \rangle = & \left[\begin{array}{c} \text{Diagram 1} + \text{Diagram 2} + \text{Diagram 3} \\ + \text{Diagram 4} + \text{Diagram 5} + \text{Diagram 6} + \text{Diagram 7} \\ + \text{Diagram 8} + \text{Diagram 9} + \text{Diagram 10} + \dots \end{array} \right] f_0
\end{aligned} \tag{75}$$

It is not difficult to see that the sum in the bracket on the r.h.s. of Eq. (75) is just $i\Gamma_0$ i.e., the limit of $i\Gamma_k$ of Eq. (21) when k goes to zero (here we note that the last vertex is $\hat{L}(k)$ instead of $\hat{L}(-k)$). Hence there is a minus sign compared to the diagrammatical rule of $(-i\Gamma_k)$ in Eq. (21), which the conservation of momentum requires. This minus sign can be factorized out. We get the $i\Gamma_0$ instead of $-i\Gamma_0$). This is true to any higher order because the diagrammatical structure of f_k (the fundamental constructive diagram, see Appendix D) suggests that all diagrams of $\hat{L}(k) \langle \phi_k^* f_k \rangle$ must be overlapping and include all possible connecting ways. It is obvious for $\hat{L}(k) \langle \phi_k^* f_k^{(c)} \rangle$ because there is only one wiggly line in $f_k^{(c)}$ to be connected. The same case is also applied to $\hat{L}(k) \langle \phi_k^* \tilde{f}_k \rangle$, although there are many wiggly lines in \tilde{f}_k , by noting that these wiggly lines are uncorrelated with each other. Therefore, we arrive at an important result

$$\sum_k \hat{L}(k) \langle \phi_k^* f_k \rangle = i\Gamma_0 f_0. \tag{76}$$

The transport equation Eq. (72) becomes

$$(\partial_t + \vec{v} \cdot \nabla + \Gamma_0) f_0 = 0. \tag{77}$$

Because the derivatives $\partial/\partial \vec{v}$ at the extreme right and left can always be extracted from Γ_0 , Eq. (77) is readily written in form as

$$\left[\partial_t + \vec{v} \cdot \nabla + \left(\frac{q}{m} \right)^2 \vec{\partial} \cdot \overleftrightarrow{D} \cdot \vec{\partial} \right] f_0 = 0, \tag{78}$$

where the formal diffusion tensor \overleftrightarrow{D} is defined as

$$\Gamma_0 \equiv \left(\frac{q}{m} \right)^2 \vec{\partial} \cdot \overleftrightarrow{D} \cdot \vec{\partial}. \tag{79}$$

In fact, infinite derivatives to \vec{v} are contained in \overleftrightarrow{D} . The infinite series of derivatives to \vec{v} could be truncated only if the non-local effect in the velocity space is not important.

The manifest Markovian form of the transport equation [Eq. (78)] is attributed to the homogeneity in space and time which we have assumed to manipulate the fluctuating equations. A multiscale method has been developed to obtain a non-Markovian form of the transport equation and will be seen elsewhere.

VII. Energy Conservation in Electrostatic Drift Waves

As pointed out in previous sections the violation of energy conservation from the resonance broadening theory will survive if the modification due to renormalized averaged distribution function to the second order is considered as done in Dupree and Tetrault's prescription⁶ and similar versions by other authors.¹⁷ This problem will be analyzed and generalized in this section to show that the perturbation theory proposed in this paper satisfies the energy conservation order by order. This might be interesting because any attempt beyond the DIAC with diffusion approximation, which is equivalent to second order of perturbation of this paper without incoherent part, should satisfy this kind of energy conservation. However, this is not shown successfully before. For simplicity, only the shearless slab model is considered. The generalization to a sheared slab model is straightforward.

Using the Vlasov equation for a guiding center in uniform magnetic field, we write the perturbed distribution function in Fourier representation, as done similar to Sec. II, as

$$f_k = G_k \hat{L}_0(k) f_0 \Phi_k + G_k \sum_{k_1} \hat{L}(k, k_1) \Phi_{k_1} f_{k-k_1} + G_k i \Gamma_k f_k \quad (80)$$

where

$$\begin{aligned} \hat{L}_0(k) &\equiv -(e/T_e)(k_{\parallel} v_{\parallel} - \omega_{*}^{(e)}) \\ \hat{L}(k, k_1) &\equiv (e/m) k_{1,\parallel} \partial_{\parallel} - i(c/B_0)(\vec{k} \times \vec{k}_1) \cdot \vec{b}_0 \\ G_k &= (\omega - k_{\parallel} v_{\parallel} + i \Gamma_k)^{-1}. \end{aligned}$$

The power done by drift current is expressed as¹⁷

$$\langle \vec{j}_{\perp} \cdot \vec{E}_{\perp} \rangle = ie \int dv_{\parallel} dk G_k^{(0)-1} \langle f_k \Phi_k^{*} \rangle \quad (81)$$

where

$$G_k^{(0)-1} \equiv \omega - k_{\parallel} v_{\parallel}.$$

Substituting $f_k = \mathcal{A}\phi_k + \tilde{f}_k$ and $G_k^{(0)-1} \equiv G_k^{-1} - i\Gamma_k$ into Eq. (81), we have

$$\begin{aligned} \langle \vec{j}_{\perp} \cdot \vec{E}_{\perp} \rangle = ie \int dv_{\parallel} dk \Big\{ & \langle \phi_k^* G_k^{-1} \mathcal{A}\phi_k \rangle + \langle \phi_k^* (-i\Gamma_k) \mathcal{A}\phi_k \rangle \\ & + \langle \phi_k^* G_k^{-1} \tilde{f}_k \rangle + \langle \phi_k^* (-i\Gamma_k) \tilde{f}_k \rangle \Big\}. \end{aligned} \quad (82)$$

All four terms on the r.h.s. of Eq. (82) can be expressed by connected diagrams. For convenience, we firstly prove the following two useful lemmata.

Lemma I

In a given diagram if there are two wiggly lines k and k_1 which connect to the highest vertex, then if the two wiggly lines intersect at a multi-wave vortex, the contribution of this diagram to Eq. (69) vanishes (Fig. 3).

Proof

The part relevant to k and k_1 in the diagram can be written as $\hat{L}(k, k_1)P(k - k_1)\phi_{k_1}\phi_k^*$. For the highest vertex, the contribution from the explicit velocity derivative of $\hat{L}(k, k_1)$, $\hat{L}_1(k, k_1) \equiv (e/m)k_{1,\parallel}\partial_{\parallel}$, becomes zero after the integration over v_{\parallel} . The contribution from the second part also vanishes

$$\hat{L}(k, k_1) \rightarrow \hat{L}_2(k, k_1) \equiv -i \left(\frac{c}{B_0} \right) (\vec{k} \times \vec{k}_1) \cdot \vec{b}_0$$

as $\hat{L}_2(k, k_1)$ changes its sign under a transformation ($k \leftrightarrow -k_1$) whereas $k - k_1$, and $\phi_k\phi_{k_1}^*$ are invariant under this transformation.

We define the two diagrams to be adjoint with each other, if they have the same highest vertex $\hat{L}(k, k_1)$ where the two wiggly lines k and k_1 meet, and the remaining parts of the two diagrams transform into each other through the operation ($k \leftrightarrow -k_1$). A few examples are illustrated in Fig. 4 and Fig. 5

Lemma II

The sum of the contribution of the adjoint diagrams to the integral in Eq. (69) is equal to zero.

Proof

For the highest vertex the contribution from \hat{L}_1 is trivially zero. The contribution from $\hat{L}_2(k, k_1)$ terms vanishes as the $\hat{L}_2(k, k_1)$ vertex changes sign under the transformation ($k \leftrightarrow -k_1$) while the remaining parts of the sum of the diagrams are unchanged.

We shall show the energy conservation of the first few orders explicitly by using the above two lemmata.

To zero order there is only one contribution from $\langle \phi_k^* G_k^{-1} \mathcal{A} \phi_k \rangle$, which is linear one $\sim \hat{L}_0 f_0$. It changes its sign under k -inversion and thus gives no contribution in the integration over k .

To the first order there is only one contribution from the incoherent source $\langle \phi_k^* G_k^{-1} \tilde{f}_k \rangle$ (Fig. 6). It gives no contribution owing to Lemma I.

In the second order, besides the contribution from $\langle \phi_k^* G_k^{-1} \tilde{f}_k \rangle$ (Fig. 7), which vanishes owing to Lemma I. There are two additional terms [Fig. 8; (a) and (b)]. One term comes from $\langle \phi_k^* G_k^{-1} \mathcal{A} \phi_k \rangle$ (Fig. 8(a)), the other from $\langle \phi_k^* (-i\Gamma_k) \mathcal{A} \phi_k \rangle$ (Fig. 8(b)). The sum of these two terms is cancelled with each other according to Lemma II. The violation of energy conservation would occur if we had only kept the resonance broadening in $i\Gamma_k$ while ignoring the modification in the renormalized averaged distribution function (represented by \mathcal{A} here). This is no other than the mismatching in perturbation theory to second order. Therefore, Dupree and Tetrault's prescription for the energy conservation is just a manifestation as to how to obtain a correct perturbation theory to the second order. However, within the second order whether or not correct for the incoherent part is irrelevant owing to the Lemma I. As we shall see below, to the third order the correct form of the incoherent part is indeed relevant in the energy conservation, which becomes a crucial test to any progress beyond the Dupree and Tetrault's theory.

To third order $\langle \phi_k^* (-i\Gamma_k) \tilde{f}_k \rangle$ (Fig. 9(a)) gives a term which cancels its adjoint

term in $\langle \phi_k^* G_k^{-1} \mathcal{A} \phi_k \rangle$ (Fig. 9(b)). At the same time $\langle \phi_k^* G_k^{-1} \mathcal{A} \phi_k \rangle$ gives another term (Fig. 4(a)) which is cancelled by the nonzero term in $\langle \phi_k^* G_k^{-1} \tilde{f}_k \rangle$ (Fig. 4(b)).

The terms in Fig. 5(a) come out of $\langle \phi_k^* (-i\Gamma_k) \mathcal{A} \phi_k \rangle$, which is cancelled by its adjoint term in Fig. 5(b) out of $\langle \phi_k^* G_k^{-1} \tilde{f}_k \rangle$. The full cancellation to the third order is thus shown explicitly. We stress at this point that the incoherent source and the non-Gaussian part should be taken into account simultaneously to survive the energy conservation. This implies that the DIAC must violate the energy conservation where the polarization part is taken into account while the incoherent part is neglected.

The energy conservation to the fourth order is shown explicitly (in diagram) in Appendix E.

A rather lengthy proof of the energy conservation up to arbitrary higher order has been succeeded based on the above two lemmata and other fourteen lemmata concerning the topological structure of the diagrams involved in the four terms of Eq. (82). For the limited scope of this paper we neglect them.*

VIII. The Spectrum Equations to Second Order Perturbations

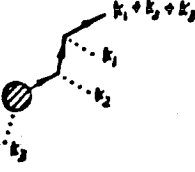
From a point of view of perturbation theory the lowest order of the incoherent source should be more important than the modification of the renormalized average distribution function. The validity of ignorance of those terms is justified if either only the production of energy is concerned or the phase space for three wave interaction is very small. However, the role of incoherent source will become more significant in the determination of spectrum, if the phase space of three wave interaction is not very small at the saturated level of turbulence. Provided $e\phi/T$ is small enough to be a perturbative parameter. A closed set of spectrum equations can be constructed from the renormalized perturbation theory of the paper.

To the second order the nonlinear Poisson equation, [Eq. (29)] is reduced to

$$\epsilon_k^{(c)} \phi_k = \sum_{k_1+k_2=k} \tilde{\epsilon}_{k_1, k_2}^{(2)} \phi_{k_1} \phi_{k_2} + \sum_{k_1+k_2+k_3=k} \tilde{\epsilon}_{k_1, k_2, k_3}^{(3)} \phi_{k_1} \phi_{k_2} \phi_{k_3} \quad (83)$$

* For interested readers, a copy containing details of the proof to arbitrary order will be offered on request to the author.

where $\epsilon_k^{(c)}$ is given by Eq. (62), $\tilde{\epsilon}_{k_1, k_2}^{(2)}$ is given by Eq. (66) and

$$\tilde{\epsilon}_{k_1, k_2, k_3}^{(3)} \equiv \Phi_{k_1+k_2+k_3}$$


$$= -\frac{4\pi q}{|\vec{k}_1 + \vec{k}_2 + \vec{k}_3|^2} \int d\vec{v} G_{k_1+k_2+k_3} \hat{L}(k_1) G_{k_2+k_3} \hat{L}(k_2) G_{k_3} \hat{L}(k_3) f_0. \quad (84)$$

Multiplying ϕ_k^* on both sides of Eq. (83) and ensemble averaging yield

$$\epsilon_k^{(c)} I_k = \sum_{k_1+k_2=k} \tilde{\epsilon}_{k_1, k_2}^{(2)} \langle \phi_{k_1} \phi_{k_2} \phi_k^* \rangle + \sum_{k_1+k_2+k_3=k} \tilde{\epsilon}_{k_1, k_2, k_3}^{(3)} \langle \phi_{k_1} \phi_{k_2} \phi_{k_3} \phi_k^* \rangle. \quad (85)$$


In a quasi-Gaussian process the correlation $\langle \phi_{k_1} \phi_{k_2} \phi_{k_3} \phi_k^* \rangle$ on the r.h.s. of Eq. (85) becomes zero because of the incorrelation between ϕ_{k_1} , ϕ_{k_2} , ϕ_{k_3} , and

$$\langle \phi_{k_1} \phi_{k_2} \phi_k^* \rangle = 2 \frac{\tilde{\epsilon}_{k_1, k_2}^{(2)*}}{\epsilon_k^*} I_{k_1} I_{k_2} + 2 \frac{\tilde{\epsilon}_{-k_1, k}^{(2)}}{\epsilon_{k_2}} I_{k_1} I_k + 2 \frac{\tilde{\epsilon}_{-k_2, k}^{(2)}}{\epsilon_{k_1}} I_{k_2} I_k. \quad (86)$$

Then, Eq. (85) becomes

$$\left[\epsilon_k^{(c)} - 4 \sum_{k_1} \frac{\tilde{\epsilon}_{k_1, k-k_1}^{(2)} \tilde{\epsilon}_{-k_1, k}^{(2)}}{\epsilon_{k-k_1}} I_{k_1} \right] I_k = 2 \sum_{k_1+k_2=k} \frac{|\tilde{\epsilon}_{k_1, k_2}^{(2)}|^2}{\epsilon_k^*} I_{k_1} I_{k_2}. \quad (87)$$

On the other hand, to the second order we already have an equation for G_k and I_k [Eq. (21)].

$$-i\Gamma_k = \text{cloud diagram} = \sum_{k_1} \hat{L}(k_1) G_{k-k_1} \hat{L}(-k_1) I_{k_1} = G_k^{(0)-1} - G_k^{-1} \quad (88)$$


where $G_k^{(0)-1} \equiv G_k^{-1} - i\Gamma_k$, the inverse bare propagator.

Eqs. (87) and (88) are combined together to give a closed set of equations for G_k and I_k , because the other items in the equations like f_0 , $\hat{L}(k)$, $G_k^{(0)}$ are known quantities. They are quite similar to the equations proposed by Biskamp²¹ in diagrammatical technique and Orzag and Kraichnan.¹⁵

If the turbulence level is so small that Eq. (88) is approximated by $G_k^{-1} \sim G_k^{(0)-1}$, to the $O(I^2)$ Eq. (87) is then reduced to the standard spectrum equation in weak turbulence

theory, where Eq. (69) is used for the expression of $\epsilon_k^{(c)}$. In a sense the set of Eqs. (87) and (88) is the renormalized version of weak turbulence theory, in which the resonance broadening, the three wave interaction and the nonlinear scattering are all included in a consistently renormalized way.

For small, but finite I_k Eq. (88) is approximated by the single renormalization,³

$$G_k^{-1} \sim G_k^{(0)-1} - \sum_{k_1} \hat{L}(k_1) G_{k-k_1}^{(0)} \hat{L}(-k_1) I_{k_1}. \quad (89)$$

Substitution of Eq. (89) into Eq. (87) yields a spectrum equation for I_k only. The back-reaction of particle on waves is contained in the spectrum equation.

The detailed solution of Eqs. (87) and (88) in specific circumstances is not the aim of the paper. However, we should point out that the spectrum equations given in this section are a more appropriate approximate description, if the spectrum is peaked up, whereupon the clump model⁷ does not apply very well.

In the conventional perturbative approach or the diffusion approximation of the DIAC the resonance broadening [equivalent to Eq. (88)] and the nonlinear dispersion relation $\epsilon_k = 0$ have been established. The new information given in Eq. (87) is the addition of two other effects: the renormalized three-wave interaction and the renormalized nonlinear scattering.²¹

IX. Concluding Remarks

The renormalized perturbation theory presented in this paper aims at how to establish a matched perturbation theory for the Vlasov-Poisson system. The concept of matching or “order” is elucidated through the following points.

- (i) A well-defined procedure of iterative and the contents of each order.
- (ii) The proof of the renormalizability, i.e., to each order the counter term should not appear at the final perturbative expansion of f_k .
- (iii) The energy conservation is valid to each order.

In all three points the propagator is regarded as the non-perturbative quantity, otherwise the theory would reduce to the unrenormalized one.

We have seen that the violation of energy conservation is caused by the mismatching in the second order as depicted in Sec. VII. Also, we have seen in Sec. V and Sec. VII that correct weak turbulence limit did not follow from the earlier perturbative approach because the incoherent part which contributes to the first order of perturbation is not manipulated in a perturbative way or ignored at all, while the propagator and the averaged distribution function are renormalized to the second order. The critique to the perturbative approach is then answered by resorting to the matched perturbation procedure presented in this paper. In a sense the theory can be regarded as a continuation and accomplishment of the previous perturbative approach initiated by Dupree¹ and then, developed by Rudakov and Tsytovich,³ Dupree and Tetreault.⁶

In a comparison to the non-perturbative approach (the DIA)¹² we find that the two theories are somewhat different. In the original MSR systematology the Green function of kinetic equation is a two-component function, the response function R and the correlation function C ,¹³ while the so-called propagator G is generally not the Green function of Vlasov equation by its definition (as usual, a Green function is defined as source function through the formal solution of the fluctuating distribution function). On the other hand, the propagator used in the perturbative approach is indeed the Green function of Vlasov equation. It is not surprising that the renormalized propagators of the two theories are different even to the lowest non-trivial order, as the polarization part in the DIA does

contribute to this order. In view of intrinsic difference of these two theories we can not conclude which theory is superior to the other before any evidence is made manifestly.

The renormalization procedure may not need to be unique. However, the present theory does have different consequences from the DIA. For example, a Krammer-Kronig kind dispersion relation for Γ_k can be derived owing to the causality of our Green function G_k .²³ This property is non-existent in the DIA's approach.

Another emphasis is just on the role of incoherent source for the comparison to conventional perturbative approach. As is well known, only the coherent part is dealt with in perturbative approach, while the incoherent part is mainly manipulated by the clump model.⁷⁸ This semi-perturbation theory is plausible only if the spectrum is broad enough so that the granulation in phase space becomes evident. The earlier treatment by the concept of non-linear dispersion relation is basically dealing with the Compton scattering.^{6,20,9} The nonlinear scattering and the three wave interaction related with the incoherent source will cause a broadening of ω to a given \vec{k} (in a few literature it is called the "correlation broadening"). Thus to the second order of perturbation, the usual nonlinear dispersion relation $\epsilon_k^{(c)} = 0$ should be reformed. Approximately, the requirement of minimum $\epsilon_k^{(c)}$ might make sense as a substitute for the usual nonlinear dispersion relation. The condition of minimum $\epsilon_l^{(c)}$ produces a turbulence-level-dependent shift from the frequency predicted by the linear dispersion relation. In this sense the reconstructed nonlinear dispersion relation $\omega = \omega(\vec{k})$, determined by $\delta\epsilon_k^{(c)}/\delta\omega = 0$ is referred to the nonlinear mode if the Compton scattering is dominant. More precisely, a closed set of spectrum equations is established to second order [Sec. VII] in a sense of the renormalized perturbation theory. This approach suggests an alternative to clump model in solving the spectrum problem.

Another shift given by the paper is the nonlinear shift in the propagator accompanying the Dupree damping [see the end of Sec. 3]. However, we must have $\lim_{k \rightarrow 0} \text{Im}\Gamma_k = 0$, as indicated by the reality of Eq. (64), i.e., the limit of the nonlinear shift at low frequency must go to zero.

Recently, the results from simulation indicates the importance of a non-Gaussian process.²⁴ Indeed, the non-Gaussian contribution of the propagator and the coherent distribution function starts at the third order of perturbation [as seen in Eqs. (21) and (25)].

Meanwhile, the contribution from the incoherent distribution function including a non-Gaussian diagram appears at the fourth order of perturbation [see Eq. (26)]. However, it should be emphasized here that the non-Gaussian effect of the incoherent part usually begins at lower order than fourth. An example can be seen from Eq. (74), in which the first order of the incoherent part combined with other quantities gives the third order of non-Gaussian $i\Gamma_0$. The non-Gaussian effects keep a very close relationship with the incoherent part, as analyzed in Sec. VII. But, we have seen the influence of the incoherent part on the transport equation in a glance at the structure of Γ_0 . The lowest non-Gaussian structure of Γ_0 is just produced by the lowest incoherent distribution function.

Acknowledgments



The author is deeply grateful to Professor H.L. Berk for his instructive discussions on the theory as well as his great effort in the modifications of the original English version. The author is also grateful to Professor W. Horton Jr. for his detailed discussion and to P. Similon for his discussion. The latter part of this work was supported by the U.S. Department of Energy Contract DE-FG05-80ET-53088.

Appendix A

Diagrammatic Rules

Because of the importance of the diagrammatic scheme introduced in this paper, a detailed account of the diagrammatic rules is given in this appendix.

In each diagram like in Fig. 10 or 11, the solid line represents the propagator G_k , [Fig. 10(a)] with k denoting the four-momentum of the particles carried by the propagator. The one exception to this representation is when the solid line is at the lowest part of the diagram which then represents the fluctuating distribution function f_{k-k_1} [Fig. 10(b)] or function f_k [Eq. (7),(8)].

There is always an arrow to denote the direction of its k . The solid line deflects whenever it meets a wiggly line [Fig. 10(c)] which represents wave ϕ_{k_1} . The redirection indicates that there is a vertex \hat{L} which is called wave particle interaction vertex implying their interaction. At the vertex there must be conservation of momentum. When the wiggly line of momentum k_1 is an external line, which one end connecting with the solid line of momentum k at the vertex the other end being free, the momentum connected with it is taken up by the solid line below the vertex has a momentum $k - k_1$. The vertex at the intersection between solid line and wiggly line is an operator, which generally does not commute with the propagator G . At the end of the lowest solid line it may be connected to a shaded bubble  $\equiv \hat{L}_0(k)f_0$ or it may be open ended. In the latter case this lowest solid line means $f_{k'}$. A circle  is introduced here to denote $i\Gamma_k$. The wiggly line which connects two vertices is called an internal line and it denotes $|\phi_k|^2$. Sometimes several wiggly lines meet at one point. The point is called multiwave vertex. There is no interaction at a multiwave vertex akin to the interaction \hat{L} at the wave-particle vertex. However, the multiwave vertex provides the conservation of four-momentum of waves $k_1 + k_2 + \dots + k_n = 0$ where k_1, k_2, \dots, k_n are the four-momentum of waves connected to the multiwave vertex. Both the internal line and the multiwave connecting wiggly lines imply a non-fluctuating closed structure for the correlation of corresponding waves.

A summation index with parenthesis, (k_i) , means $k_i \neq k$ (k is the coherent momentum) and the designated wiggly line by (k_i) is uncorrelated with other wiggly lines designated by momentum with parenthesis in the same diagram. A typical example of this

diagrammatical rule is given in Fig. 11 which corresponds to the following formula:

$$\begin{aligned}
& G_k \sum_{k_1} \hat{L}(k_1) G_{k-k_1} \sum_{(k_2)} \hat{L}(k_2) G_{k-k_1-k_2} \sum_{k_3} \hat{L}(k_3) G_{k-k_1-k_2-k_3} \hat{L}(-k_1) \\
& G_{k-k_2-k_3} \sum_{k_5} \hat{L}(k_5) G_{k-k_2-k_3-k_5} \sum_{k_6} \hat{L}(k_6) G_{k-k_2-k_3-k_5-k_6} \hat{L}(-k_3-k_5) \\
& G_{k-k_2-k_6} \hat{L}(k-k_2) G_{-k_6} \hat{L}(-k_6) f_0 \left\langle \left\langle \phi_{k_1} \phi_{k_1}^* \right\rangle \right\rangle \left\langle \left\langle \phi_{k_6} \phi_{k_6}^* \right\rangle \right\rangle \left\langle \left\langle \phi_{k_3} \phi_{k_5} \phi_{k_3+k_5}^* \right\rangle \right\rangle \phi_{k_2} \phi_{k-k_2}.
\end{aligned}$$

Appendix B

Correlation Expansion

In the perturbation a systematic procedure, named correlation expansion, is adopted based on the definition of the correlation function to all orders.

The stochastic quantities for any stochastic process, A,B,C,D... might be correlated with each other, so that we have

$$\langle A \rangle = \langle A \rangle \quad (B1)$$

$$\langle AB \rangle = \langle A \rangle \langle B \rangle + \langle \langle AB \rangle \rangle \quad (B2)$$

$$\begin{aligned} \langle ABC \rangle &= \langle A \rangle \langle B \rangle \langle C \rangle + \langle A \rangle \langle \langle BC \rangle \rangle + \langle B \rangle \langle \langle AC \rangle \rangle \\ &\quad + \langle C \rangle \langle \langle AB \rangle \rangle + \langle \langle ABC \rangle \rangle \end{aligned} \quad (B3)$$

$$\begin{aligned} \langle ABCD \rangle &= \langle A \rangle \langle B \rangle \langle C \rangle \langle D \rangle + \langle A \rangle \langle B \rangle \langle \langle CD \rangle \rangle + \langle A \rangle \langle C \rangle \langle \langle BD \rangle \rangle \\ &\quad + \langle A \rangle \langle D \rangle \langle \langle BC \rangle \rangle + \langle B \rangle \langle C \rangle \langle \langle AD \rangle \rangle + \langle B \rangle \langle D \rangle \langle \langle AC \rangle \rangle \\ &\quad + \langle C \rangle \langle D \rangle \langle \langle AB \rangle \rangle + \langle \langle AB \rangle \rangle \langle \langle CD \rangle \rangle + \langle \langle AC \rangle \rangle \langle \langle BD \rangle \rangle \\ &\quad + \langle \langle AD \rangle \rangle \langle \langle BC \rangle \rangle + \langle A \rangle \langle \langle BCD \rangle \rangle + \langle B \rangle \langle \langle ACD \rangle \rangle \\ &\quad + \langle C \rangle \langle \langle ABD \rangle \rangle + \langle D \rangle \langle \langle ABC \rangle \rangle + \langle \langle ABDC \rangle \rangle \end{aligned} \quad (B4)$$

where $\langle \langle AB \rangle \rangle$, $\langle \langle ABC \rangle \rangle$, $\langle \langle ABCD \rangle \rangle$... are called the correlation functions of stochastic quantities A,B,C,D... . They simplify the dependent probability of multiple stochastic quantities and defined as the difference of the ensemble average from the lower order ones. Having the definition of correlation functions in mind, we can expand the product of stochastic quantities A,B,C,D... in terms of correlation functions. For example,

$$AB = \langle A \rangle \langle B \rangle + \langle \langle AB \rangle \rangle. \quad (B5)$$

The quantities in parenthesis are not correlated with each other. When the ensemble average is taken over them, the average is split into that acting on each single quantity,

because the correlated part has been extracted from them, i.e., $\langle(A)(B)\rangle = \langle A\rangle\langle B\rangle$. We readily find the consistency of Eq. (B5) with Eq. (B2).

The further examples are

$$ABC = (A)(B)(C) + (A)\langle\langle BC\rangle\rangle + (B)\langle\langle AC\rangle\rangle + (C)\langle\langle AB\rangle\rangle + \langle\langle ABC\rangle\rangle \quad (B6)$$

$$\begin{aligned} ABCD = & (A)(B)(C)(D) + (A)(B)\langle\langle CD\rangle\rangle + (A)(C)\langle\langle BD\rangle\rangle \\ & + (A)(D)\langle\langle BC\rangle\rangle + (B)(C)\langle\langle AD\rangle\rangle + (B)(D)\langle\langle AC\rangle\rangle \\ & + (C)(D)\langle\langle AB\rangle\rangle + \langle\langle AB\rangle\rangle\langle\langle CD\rangle\rangle + \langle\langle AC\rangle\rangle\langle\langle BD\rangle\rangle \\ & + \langle\langle AD\rangle\rangle\langle\langle BC\rangle\rangle + (A)\langle\langle BCD\rangle\rangle + (B)\langle\langle ACD\rangle\rangle \\ & + (C)\langle\langle ABD\rangle\rangle + (D)\langle\langle ABC\rangle\rangle + \langle\langle ABCD\rangle\rangle. \end{aligned} \quad (B7)$$

A quantity in parenthesis might be correlated with the quantities not in parenthesis; however, no quantity in $\langle\langle\dots\rangle\rangle$ could be correlated with quantity outside it. In fact, the correlation expansion can be done only for part of the product. Thus we write

$$\begin{aligned} ABCD = & (A)(B)(C)D + (A)\langle\langle BC\rangle\rangle D + (B)\langle\langle AC\rangle\rangle D \\ & + (C)\langle\langle AB\rangle\rangle D + \langle\langle ABC\rangle\rangle D \end{aligned} \quad (B8)$$

The further expansion of Eq. (B8), according to the above rule, reads

$$\begin{aligned} (A)(B)(C)D = & (A)(B)(C)(D) + (A)\langle\langle BCD\rangle\rangle + (B)\langle\langle ACD\rangle\rangle \\ & + (C)\langle\langle ABD\rangle\rangle + (A)(B)\langle\langle CD\rangle\rangle + (A)(C)\langle\langle BD\rangle\rangle \\ & + (B)(C)\langle\langle AD\rangle\rangle + \langle\langle ABCD\rangle\rangle \end{aligned} \quad (B9)$$

[Only the correlation among A,B,C, is prohibited in this expansion.]

$$(A)\langle\langle BC\rangle\rangle D = (A)(D)\langle\langle BC\rangle\rangle + \langle\langle BC\rangle\rangle\langle\langle AD\rangle\rangle \quad (B10)$$

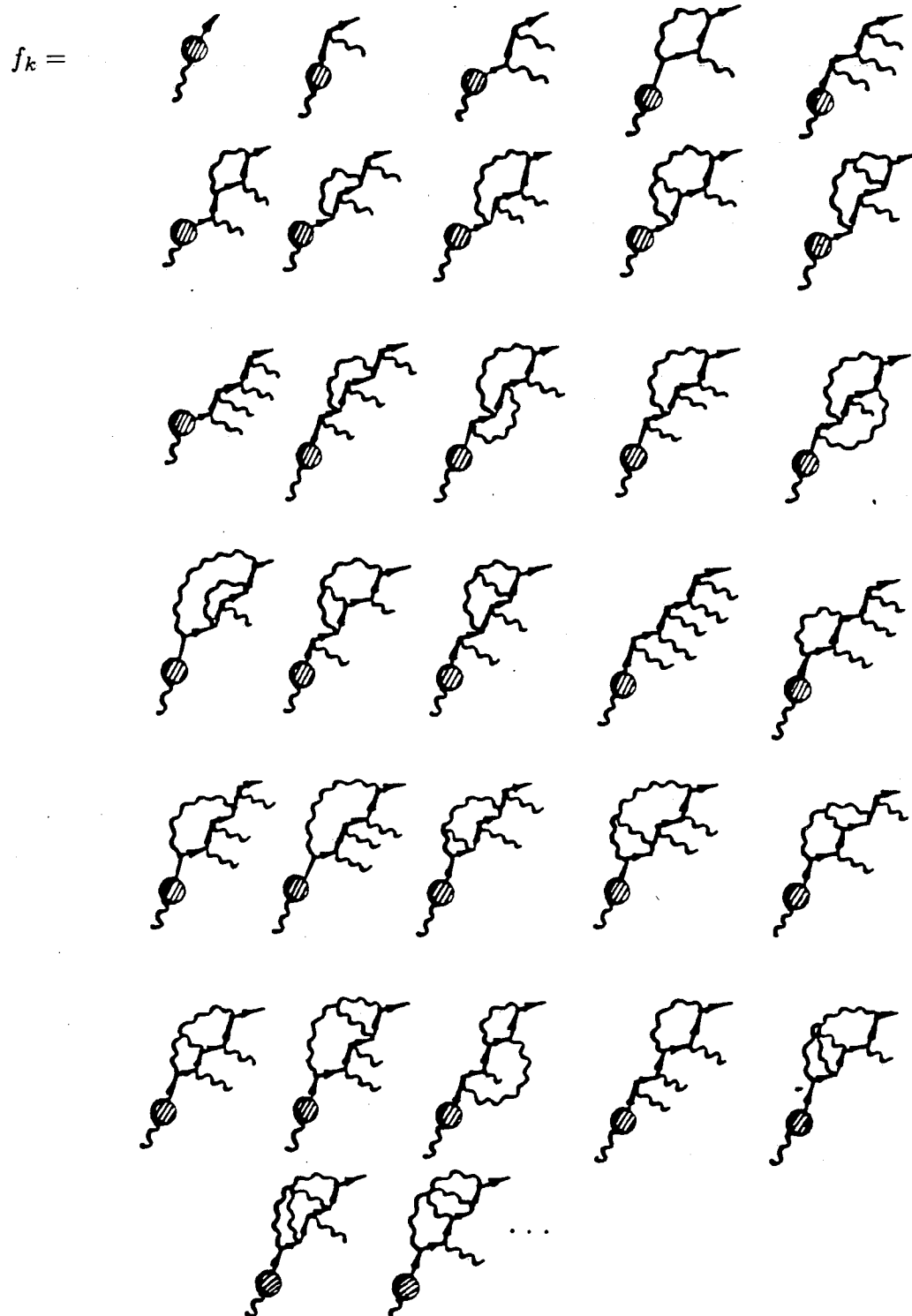
$$(B)\langle\langle AC\rangle\rangle D = (B)(D)\langle\langle AC\rangle\rangle + \langle\langle AC\rangle\rangle\langle\langle BD\rangle\rangle \quad (B11)$$

$$(C)\langle\langle AB\rangle\rangle D = (C)(D)\langle\langle AB\rangle\rangle + \langle\langle AB\rangle\rangle\langle\langle CD\rangle\rangle \quad (B12)$$

$$\langle\langle ABC \rangle\rangle D = \langle\langle ABC \rangle\rangle (D) \quad (B13)$$

When combining Eq. (B8) with Eqs. (B9)-(B13), we readily see the consistency with the result of Eq. (B7). The correlation expansion is equivalent to the cluster expansion used in the BBGKY hierarchy²⁵ and functional for both the distribution function f and the electric fields \vec{E} by virtue of the linear relations given by the Poisson equation.²⁶

Appendix C – The Perturbative of f_k to Fifth Order



In this representation the wiggly lines above the shaded bubble are uncorrelated with each other, while the wiggly line connected to the shaded bubble may or may not be correlated with the other open wiggly lines in a given diagram as discussed in Section IV.

Appendix D – Construction Rules of the Perturbative Expression

of the Coherent Terms $f_k^{(c)}$ and the Incoherent Terms \tilde{f}_k

We introduce some useful definitions first.

Definition I. Primitive frame diagram

It consists of a solid line with n wave-particle vertices, each of which connects with an open wiggly line, a shaded bubble with a wiggly line connected to the lowest end of the solid line. The four-momentum conservation holds for lines

The fourth order primitive frame diagram pertaining to each wave-particle vertex as well as for lines pertaining to the shaded bubble. Such a diagram is defined as the n th order primitive frame diagram as shown in Fig. 12.

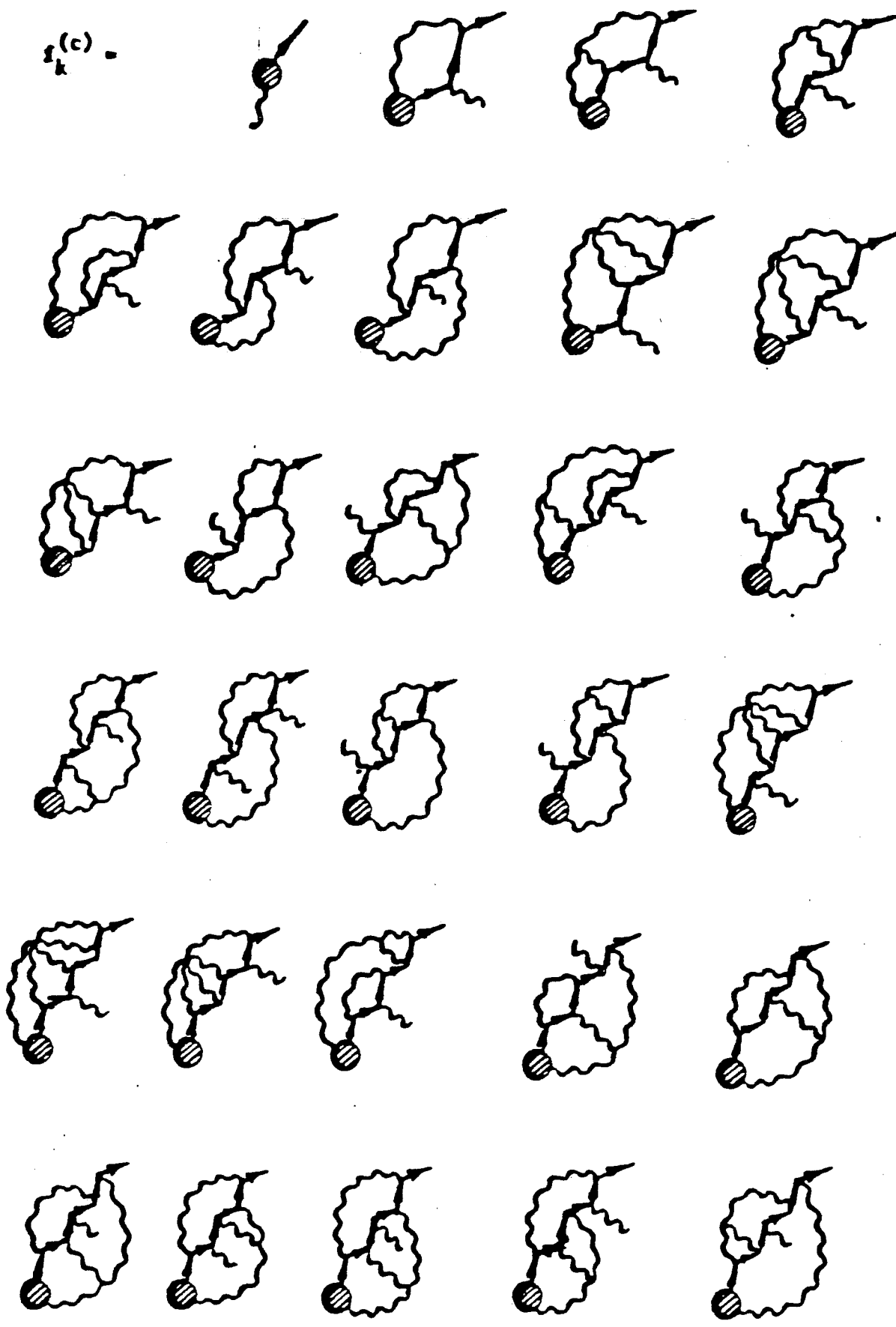
Definition II. – Fundamental constructive diagram

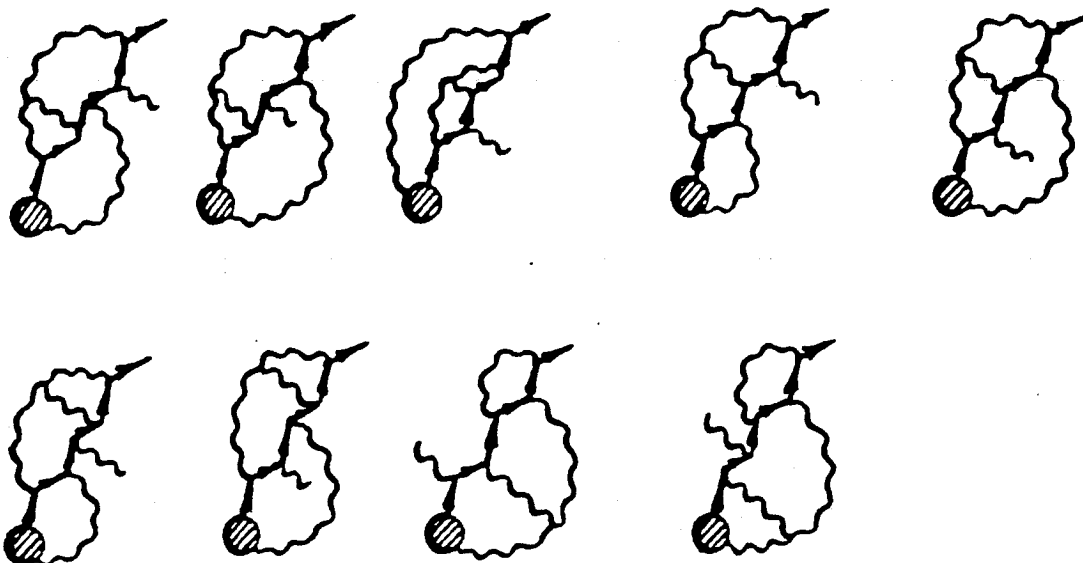
Starting with the given order primitive frame diagram we combine the wiggly lines in all possible way to form internal line and/or closed structure containing multi-wave vertex with the exception that it will cause any type of self-energy sub-structure and zero-momentum propagator in the diagram. The set of the resultant diagram is called the fundamental constructive diagram for the given order. For example, all possible fundamental constructive diagrams given by the 3rd order primitive frame diagram (Fig. 13(a)) are given in Fig. 6(b).

The formation rule of $f_k^{(c)}$

All fundamental constructive diagrams with only single open wiggly line comprise the contribution to $f_k^{(c)}$ for any given order. The diagrammatical expression of $f_k^{(c)}$ to the fifth order is illustrated as follows

$f_k^{(c)} =$



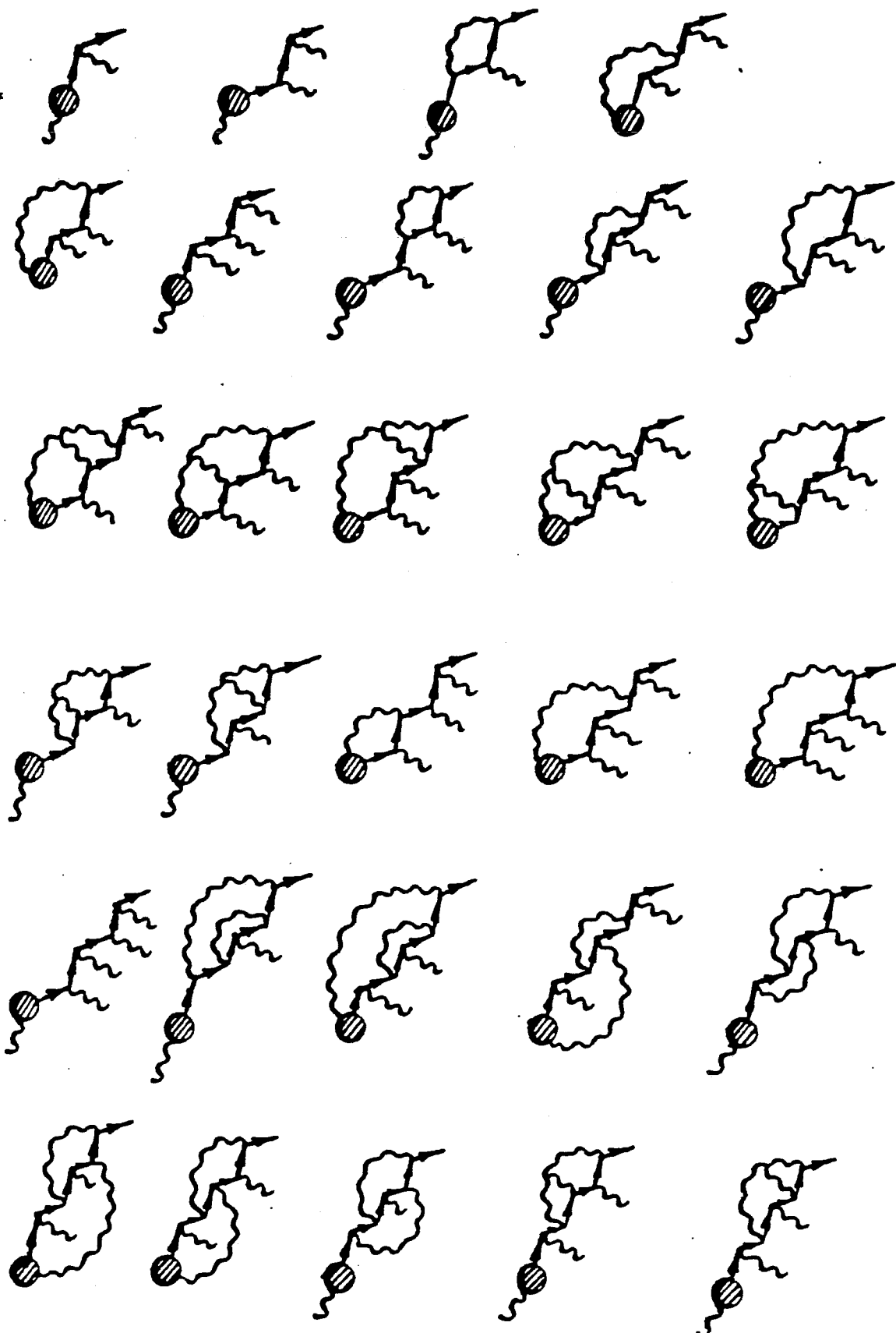


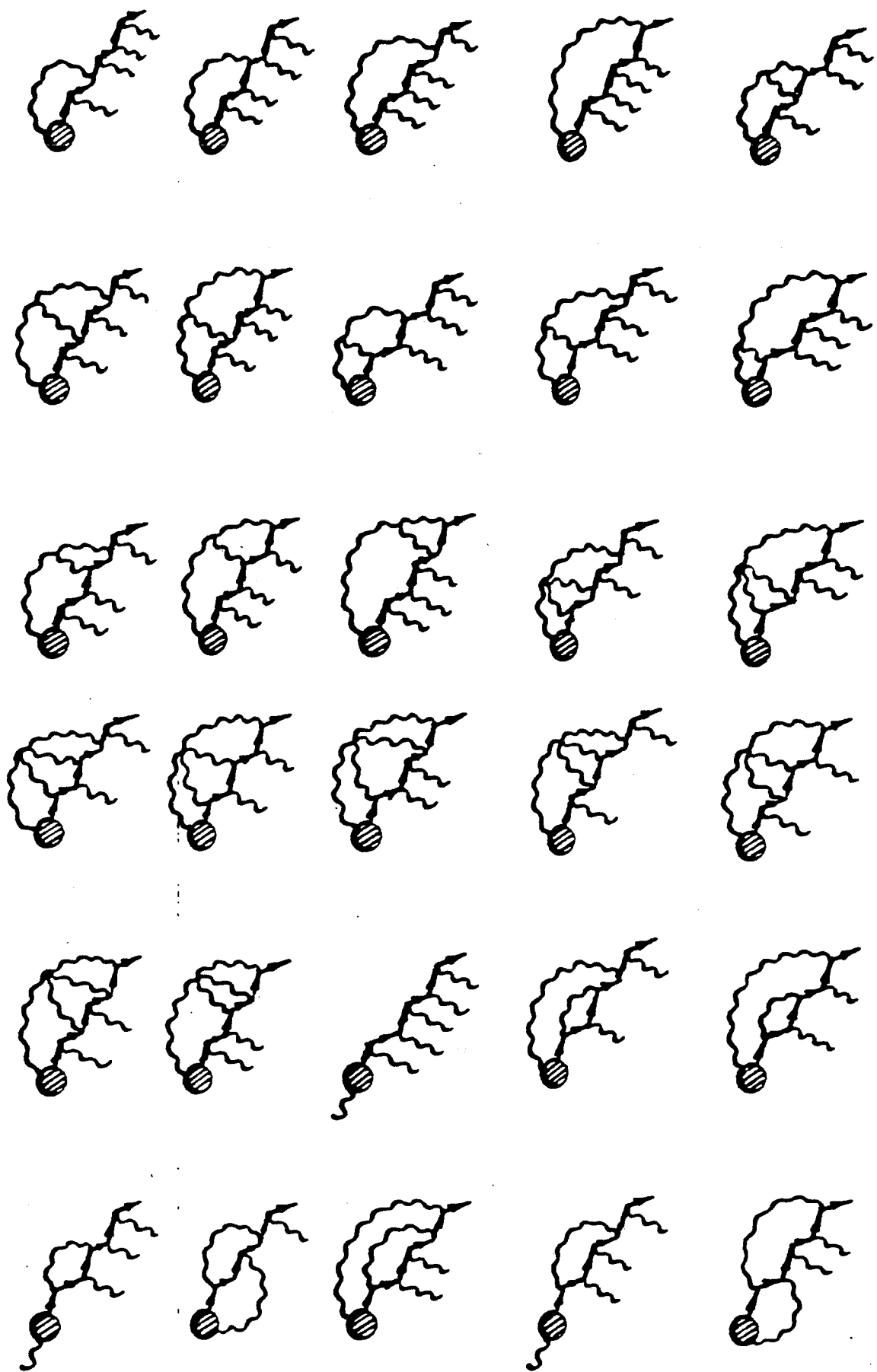
The formation rule of \tilde{f}_k

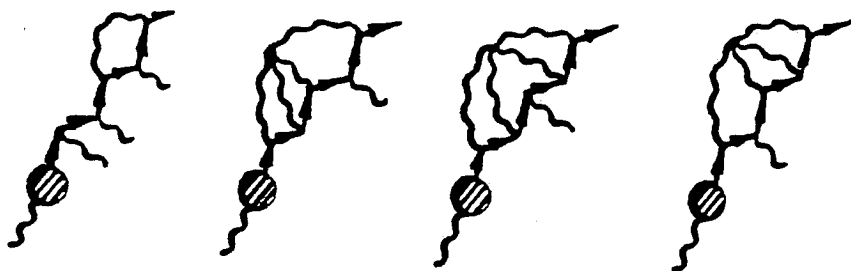
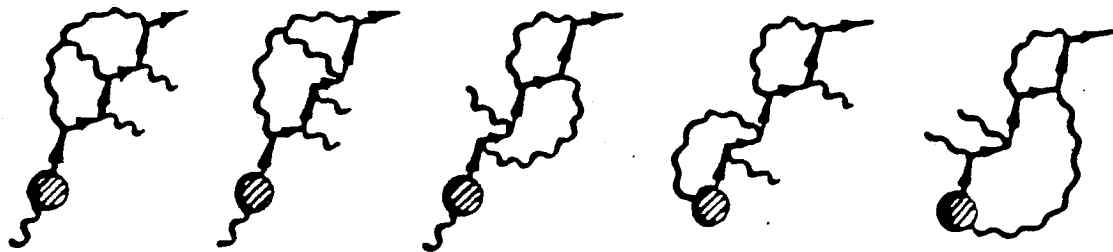
All fundamental constructive diagrams with more than one open wiggly line comprise to \tilde{f}_k for any given order. The diagrammatical expression of \tilde{f}_k to the fifth order is illustrated as follows:

$$\tilde{f}_k =$$

\tilde{I}_k







Appendix E — Adjoint Diagrams at Fourth Order

The nonzero diagrams in fourth order are given below. They are cancelled with each other according to Lemma II, while the zero diagrams, to be zero by Lemma I, are not illustrated.

The sources composed the diagrams are given on the left of each diagram. They can be found in Appendix C.

$$\langle \phi^* G_k^{-1} A \phi_k \rangle$$

$$\mathcal{A} = \text{[Diagram 1]} \longrightarrow \text{[Diagram 2]} \quad (\text{E1})$$

$$\mathcal{A} = \text{[Diagram 3]} \longrightarrow \text{[Diagram 4]} \quad (\text{E2})$$

$$\mathcal{A} = \text{[Diagram 5]} \longrightarrow \text{[Diagram 6]} \quad (\text{E3})$$

$$\mathcal{A} = \text{[Diagram 7]} \longrightarrow \text{[Diagram 8]} \quad (\text{E4})$$

$$\mathcal{A} = \text{[Diagram 9]} \longrightarrow \text{[Diagram 10]} \quad (\text{E5})$$

$$\mathcal{A} = \text{diagram} \longrightarrow \text{diagram} \quad (\text{E6})$$

$$\mathcal{A} = \text{diagram} \longrightarrow \text{diagram} \quad (\text{E7})$$

$$\langle \phi_k^* (-i\Gamma_k) \mathcal{A} \phi_k \rangle$$

$$(-i\Gamma_k) = \text{diagram} \quad \mathcal{A} = \text{diagram} \longrightarrow \text{diagram} \quad (\text{E8})$$

$$(-i\Gamma_k) = \text{diagram} \quad \mathcal{A} = \text{diagram} \longrightarrow \text{diagram} \quad (\text{E9})$$

$$(-i\Gamma_k) = \text{diagram} \quad \mathcal{A} = \text{diagram} \longrightarrow \text{diagram} \quad (\text{E10})$$

$$\langle \phi_k^* G_k^{-1} \tilde{\gamma}_k \rangle$$

$$\tilde{\gamma}_k = \text{diagram} \longrightarrow \text{diagram} \quad (\text{E11})$$

The diagram shows a shaded circle on the left connected to a wavy line. The wavy line has a branch with a vector k_1 and another branch with a vector k . An arrow points to a second diagram where the wavy line is more complex, with the shaded circle still on the left and vectors k_1 and k indicated.

$$\tilde{\gamma}_k = \text{diagram} \longrightarrow \text{diagram} \quad (\text{E12})$$

The diagram shows a shaded circle on the left connected to a wavy line. The wavy line has a branch with a vector k_1 and another branch with a vector k . An arrow points to a second diagram where the wavy line is more complex, with the shaded circle still on the left and vectors k_1 and k indicated.

$$\tilde{\gamma}_k = \text{diagram} \longrightarrow \text{diagram} \quad (\text{E13})$$

The diagram shows a shaded circle on the left connected to a wavy line. The wavy line has a branch with a vector k_1 and another branch with a vector k . An arrow points to a second diagram where the wavy line is more complex, with the shaded circle still on the left and vectors k_1 and k indicated.

$$\tilde{\gamma}_k = \text{diagram} \longrightarrow \text{diagram} \quad (\text{E14})$$

The diagram shows a shaded circle on the left connected to a wavy line. The wavy line has a branch with a vector k_1 and another branch with a vector k . An arrow points to a second diagram where the wavy line is more complex, with the shaded circle still on the left and vectors k_1 and k indicated.

$$\tilde{\gamma}_k = \text{diagram} \longrightarrow \text{diagram} \quad (\text{E15})$$

The diagram shows a shaded circle on the left connected to a wavy line. The wavy line has a branch with a vector k_1 and another branch with a vector k . An arrow points to a second diagram where the wavy line is more complex, with the shaded circle still on the left and vectors k_1 and k indicated.

$$\tilde{\gamma}_k = \text{diagram} \longrightarrow \text{diagram} \quad (\text{E16})$$

The diagram shows a shaded circle on the left connected to a wavy line. The wavy line has a branch with a vector k_1 and another branch with a vector k . An arrow points to a second diagram where the wavy line is more complex, with the shaded circle still on the left and vectors k_1 and k indicated.

$$\tilde{\Gamma}_k = \text{Diagram 1} - \text{Diagram 2} \quad (\text{E17})$$

$$\tilde{\Gamma}_k = \text{Diagram 3} - \text{Diagram 4} \quad (\text{E18})$$

$$\langle \phi_k^* (-i\Gamma_k) \tilde{f}_k \rangle$$

$$(-i\Gamma_k) = \text{Diagram 5} \quad \tilde{\Gamma}_k = \text{Diagram 6} - \text{Diagram 7} \quad (\text{E19})$$

$$(-i\Gamma_k) = \text{Diagram 8} \quad \tilde{\Gamma}_k = \text{Diagram 9} - \text{Diagram 10} \quad (\text{E20})$$

The adjoint pairs are: (4)+(8)=0, (5)+(7)=0 (6)+(9)=0 [the pairs within the coherent part], (13)+(16)=0, (14)+(17)=0, (18)+(20)=0 [the pairs within the incoherent part]; (1)+(19)=0, (2)+(11)=0, (3)+(12)=0, (10)+(15)=0 [the pairs between the coherent and incoherent part].

References

1. T.H. Dupree, Phys. Fluids **9**, 1773 (1966).
2. T.H. Dupree, Phys. Fluids **10**, 1049 (1967).
3. W. Horton, Jr., Duk-In Choi, Phys. Rept. **49**, 275 (1979).
4. A.A. Galeev, Zh. Eksp. Teor. Fiz. **59**, 1361 (1969), (Soviet Phys. JETP **30**, 737 (1970)).
5. L.I. Rudakov, V.N. Tsytovich, Plas. Phys. **13**, 213 (1971).
6. T.H. Dupree, D.J. Tetreault, Phys. Fluids **21**, 425 (1978).
7. T.H. Dupree, Phys. Fluids **21**, 783 (1978).
8. T. Boutros-Ghali, T.H. Dupree, Phys. Fluids **24**, 1839 (1981).
9. P.H. Diamond and M.N. Rosenbluth, Phys. Fluids **24**, 1641 (1981).
10. P.L. Similon and P.H. Diamond, Phys. Fluids **27**, 916 (1984).
11. B.B. Kadomtsev, Plasma Turbulence (Academic Press, Reading, Massachusetts), 1965.
12. J.A. Krommes, Handbook of Plasma Physics, Eds., M.N. Rosenbluth and R.Z. Sagdeev, Vol. 2: Basic Plasma Physics II, edited by A.A. Galeev and R.N. Sudan (Elsevier, 1984).
13. P.C. Martin, E.D. Siggia, H.A. Rose, Phys. Rev. **8**, 423 (1973).
14. R.H. Kraichnan, Phys. Fluids **8**, 575 2219 (1965).
15. S.A. Orszag, R.M. Kraichnan, Phys. Fluids **10**, 1720 (1967).
16. D.F. Dubois, M. Espedal, Plas. Phys. **20**, 1209 (1978).
17. J.A. Krommes, Phys. Fluids **23**, 736 (1980).
18. D.F. Dubois, Phys. Fluids **19**, 1764 (1976).
19. J.A. Krommes, R.G. Kleva, Phys. Fluids **22**, 2168 (1979).
20. Duk-In Choi, W. Horton, Jr., Phys. Fluids **17**, 2048 (1974).
21. D. Biskamp, Zeitschrift für Naturforschung B **23a** Heft 9, 1362 (1968).
22. V.N. Tsytovich, *Theory of Turbulent Plasma*, Consultants Bureau, (New York, 1977).
23. Y.Z. Zhang and S.M. Mahajan, Phys. Rev. **A32**, 1759 (1985).
24. R.H. Berman, D.J. Tetreault, T.H. Dupree, Phys. Fluids **26**, 2437 (1983).

25. S. Ichimaru, *Basic Principles of Plasma Physics*, (Benjamin, Reading, Massachusetts, 1973).
26. R.C. Davidson, *Method in Nonlinear Plasma Theory*, (Academic Press, New York, 1972).

Figure Captions

Fig. 1 The excluded diagrams from the contributor as self-energy.

Fig. 2 The diagram creating propagator with zero-momentum does not exist in the iteration.

Fig. 10 An illustration for the definitions of diagrammatic rules.

Fig. 11 An illustration for the diagrammatic rules.

Fig. 12 An example for the primitive frame diagram (the fourth order).

Fig. 13 (a) and (b) All possible fundamental constructive diagrams given by the 3rd order primitive frame diagram.



Fig. 1

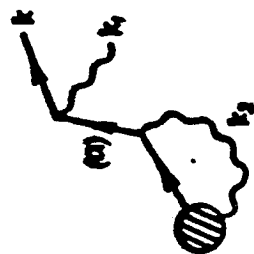


Fig. 2



Fig. 3

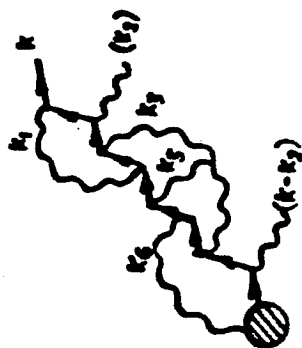


Fig. 4

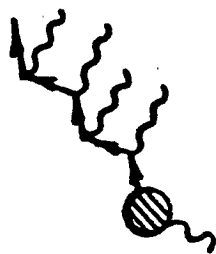


Fig. 5

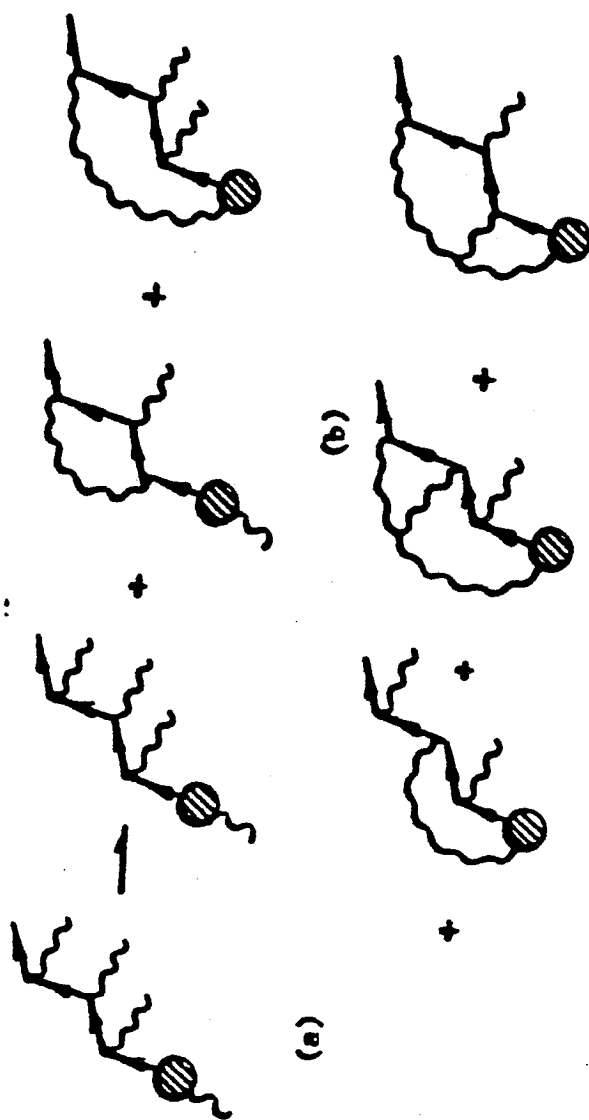


Fig. 6

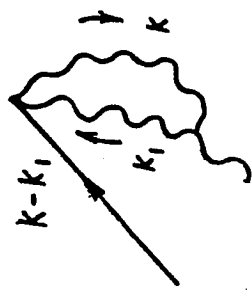
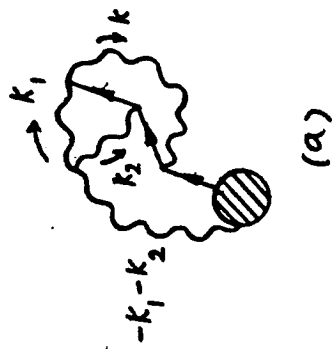
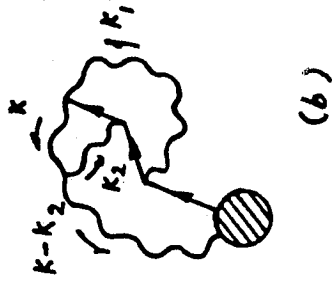


Fig 7



(a)



(b)

Fig. 8

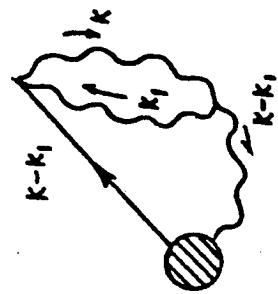
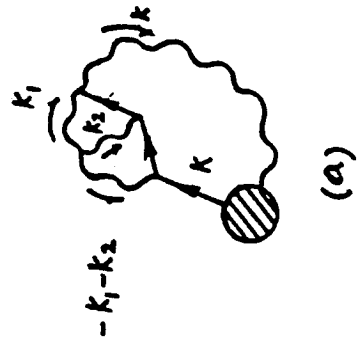


Fig. 10



(a)



(b)

Fig 9

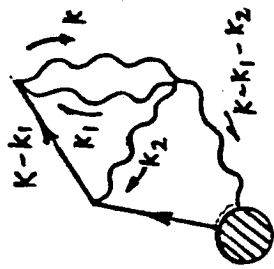
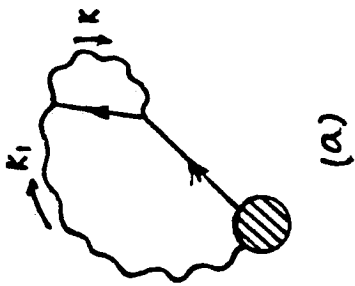


Fig. 11



(a)

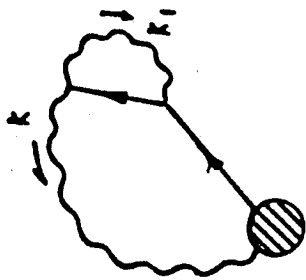
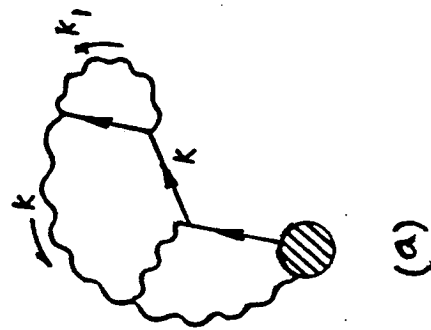
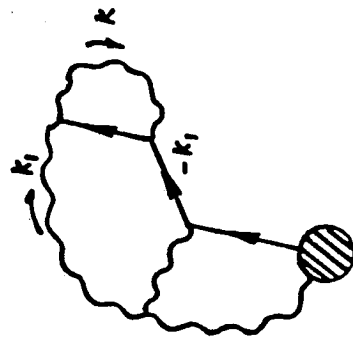


Fig. 12



(a)



(b)

Fig. 13